論文 / 著書情報
Article / Book Information

題目(和文)	
Title(English)	Investigation on brain activity related to human intention of performing a reaching movement
著者(和文)	KIMHyeonseok
Author(English)	Hyeonseok Kim
出典(和文)	学位:博士(学術), 学位授与機関:東京工業大学, 報告番号:甲第11540号, 授与年月日:2020年3月26日, 学位の種別:課程博士, 審査員:小池 康晴,金子 寛彦,中村 健太郎,八木 透,吉村 奈津江
Citation(English)	Degree:Doctor (Academic), Conferring organization: Tokyo Institute of Technology, Report number:甲第11540号, Conferred date:2020/3/26, Degree Type:Course doctor, Examiner:,,,,
学位種別(和文)	博士論文
Type(English)	Doctoral Thesis

Investigation on brain activity related to human intention of performing a reaching movement

Hyeonseok Kim

Graduate major in Human Centered Science and Biomedical Engineering

Department of Information and Communications Engineering

Tokyo Institute of Technology

Contents

Abstract

Many people have been paralyzed by many causes. The quality of their life may not be as high as a healthy person. One of the reasons is that they cannot perform a voluntary movement. In order to assist people with motor impairment, some devices such as crutches and wheelchairs have been developed and used. However, those traditional devices have a limited ability to help them. In addition, for severe patients, such low-level devices may not be helpful and high-level technology is required to help them. Up to quite recently, brain-machine interfaces (BMI) have been developed, which can cover many kinds of motor disabilities to assist people with motor disabilities. BMI system communicates with devices such as a prosthetic arm and a wheelchair to control them. It also helps people with motor disabilities to interact with the external world by providing more advanced functions to enable complex motions for example, compared to conventional assistant devices.

From a functional point of view, many kinds of motor disability can be coarsely categorized into upper-limb impairment and lower-limb impairment. Lower-limb impairment leads to walking impairment and this restricts patient's mobility. Fortunately, there are devices that can compensate it as means of transportation, and we can see them easily in our daily life. However, assistant devices for upper-limb impairment have not come into use as widely as devices for lower-limb impairment even though a prosthetic arm or exoskeletons has been developed. Upper-limb is essential for reaching and grasping that are common, natural, and fundamental tasks in daily life.

Reaching is a fundamental and essential task in daily life. Understanding how reaching movements are represented in the brain and decoding these movements are important issues in BMI research. Several studies have attempted to decode reaching movements. Compared to the number of studies on brain activity during movement execution, only a few have attempted to

classify the information before movement execution. Current many BMI systems have used brain activity during motor execution or motor imagery in which sensory input and motor command are included. The purpose of the study is to investigate brain activity during movement planning for reaching, which represents a period between target recognition and movement onset. We investigated brain activity during a planning phase for reaching movement using electroencephalography (EEG) signals. Although few previous studies have shown premovement EEG signals may be used for decoding, previous studies used only part of premovement EEG signals to show the feasibility of them.

First, we investigated whether EEG signals occurring before movement execution could be used to classify movement intention. Six subjects performed reaching tasks that required them to move a cursor to one of four targets distributed horizontally and vertically from the center. Using independent components of EEG acquired during a premovement phase, two-class classifications were performed for left vs. right trials and top vs. bottom trials using a support vector machine. Instructions were presented visually (test) and aurally (condition). In the test condition, accuracy for a single window was about 75%, and it increased to 85% in classification using two windows. In the control condition, accuracy for a single window was about 73%, and it increased to 80% in classification using two windows. Classification results showed that a combination of two windows from different time intervals during the premovement phase improved classification performance in the both conditions compared to a single window classification.

Since we confirmed the availability of premovement phase through the first experiment, we tried to find what information regarding the intended target during movement preparation is advantageous for decoding. In the second experiment, we investigated which movement parameters (i.e., direction, distance, and positions for reaching) can be decoded in premovement EEG decoding. Eight participants performed 30 types of reaching movements that consisted of 1

of 24 movement directions, 7 movement distances, 5 horizontal target positions, and 5 vertical target positions. Event-related spectral perturbations were extracted using independent components, some of which were selected via an analysis of variance for further binary classification analysis using a support vector machine. When each parameter was used for class labeling, all possible binary classifications were performed. Classification accuracies for direction and distance were significantly higher than chance level, although no significant differences were observed for position. For the classification in which each movement was considered as a different class, the parameters comprising two vectors representing each movement were analyzed. In this case, classification accuracies were high when differences in distance were high, the sum of distances was high, angular differences were large, and differences in the target positions were high. Thus, all parameters for this study may have information related to the movement, but the direction and the distance are more useful for predicting intended reaching movement than the position showing significant higher accuracy for some individuals.

Chapter 1

Introduction

1.1 Background

Many people have been paralyzed by many causes. The quality of their life may not be as high as a healthy person. One of the reasons is that they cannot perform a voluntary movement. In order to assist people with motor impairment, some devices such as crutches and wheelchairs have been developed and used. However, those traditional devices have a limited ability to help them. In addition, for severe patients, such low-level devices may not be helpful and high-level technology is required to help them.

Up to quite recently, brain-machine interfaces (BMI) have been developed, which can cover many kinds of motor disabilities to assist people with motor disabilities. BMI is often termed brain-computer interface (BCI), and the term 'BCI' has been widely used. However, BMI will be used throughout this paper. BMI system communicates with devices such as a prosthetic arm and a wheelchair to control them. It also helps people with motor disabilities to interact with the external world by providing more advanced functions to enable complex motions for example, compared to conventional assistant devices.

From a functional point of view, many kinds of motor disability can be coarsely categorized into upper-limb impairment and lower-limb impairment. Lower-limb impairment leads to walking impairment and this restricts patient's mobility. Fortunately, there are devices that can compensate it as means of transportation, and we can see them easily in our daily life. However, assistant devices for upper-limb impairment have not come into use as widely as devices for lower-limb impairment even though a prosthetic arm or exoskeletons has been developed. Upper-limb is essential for reaching and grasping that are common, natural, and fundamental tasks in daily life.

In this study, we focused on a reaching movement and investigated information for the BMI used in a reaching movement.

1.2 Brain-Machine Interface

BMIs are designed to decode neural commands from the brain and use them as input commands for external devices (Wolpaw et al., 2002; Höhne et al., 2014). Much of the development in BMIs has been to enable people with motor disabilities to interact with the external world (Mak and Wolpaw, 2009). Since brain activity can be measured directly and indirectly in many ways, a BMI system can be also categorized depending on how to measure brain activity. Thus, the BMI system can be divided into invasive BMI systems and non-invasive BMI systems.

Surgery may be required to implant electrodes for an invasive BMI system, but it provides us the high-quality signals since the position of electrodes are close to current source and measured signals are less attenuated by brain tissues (Waldert, 2016). The invasive BMI system uses intracranial neural signals such as local field potential(LFP) and electrocorticography (ECoG). As non-invasive methods require surgery, there are several risks such as infection, intracranial hemorrhage, and the possibility that electrodes hurt brain tissues. Thus, their applications are limited.

LFPs are a neural signal generated by summed extracellular potentials of individual neurons in some regions, as shown in Figure 1.1. LFPs measured around the primary motor cortex and dorsal premotor cortex enabled macaques to control a cursor (Stavisky et al., 2015). Also, when we use LFPs in long-term, they are advantageous to better reliability and sustained performance than potentials by a single-unit (Flint et al., 2013).

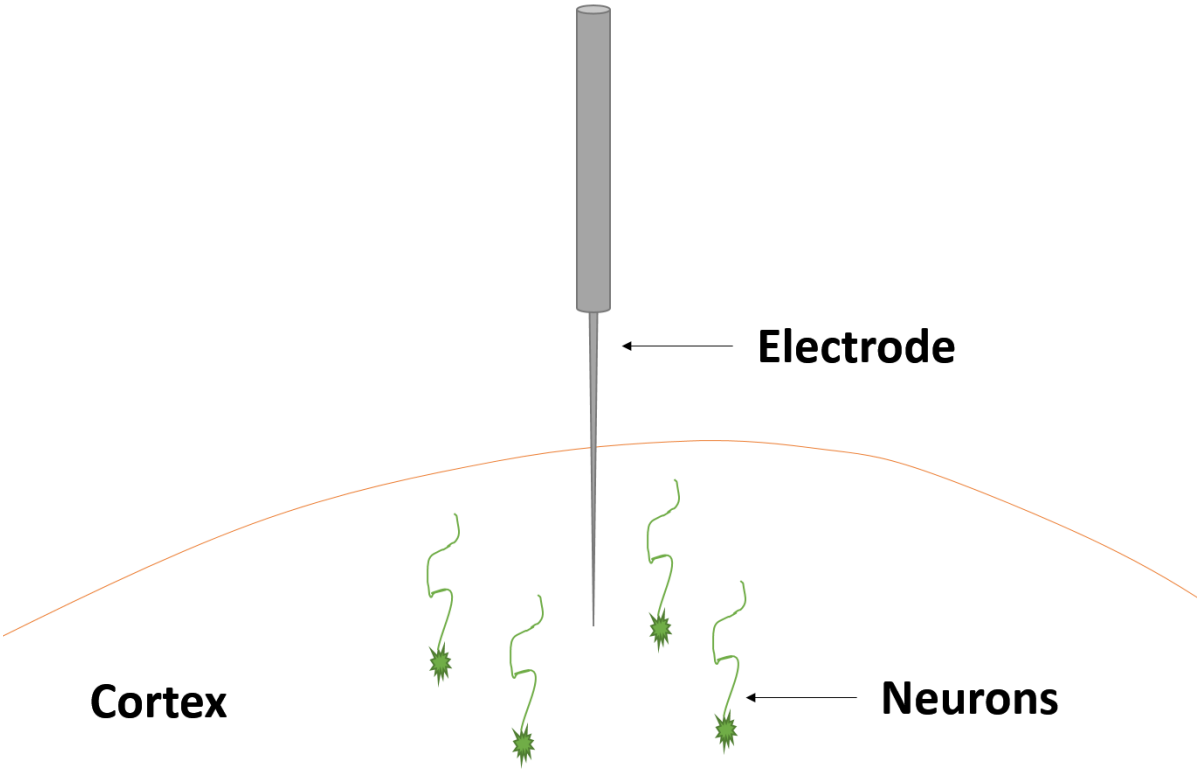

Figure 1.1: Measurement of local field potentials.

ECoG measures electrophysiological signals with electrodes above the dura mater or below the dura mater, so it does not require to penetrate the cerebral cortex. The electrode array is typically used to measure ECoG signals, as shown in Figure 1.2. ECoG also has been used for BMI system to control a cursor (Leuthardt et al., 2004), predict finger positions (Acharya et al., 2010), and control an upper limb prosthesis (Fifer et al., 2012). However, research in humans using ECoG has been limited and many studies have been performed in animals because surgery is required (Schal et al., 2011).

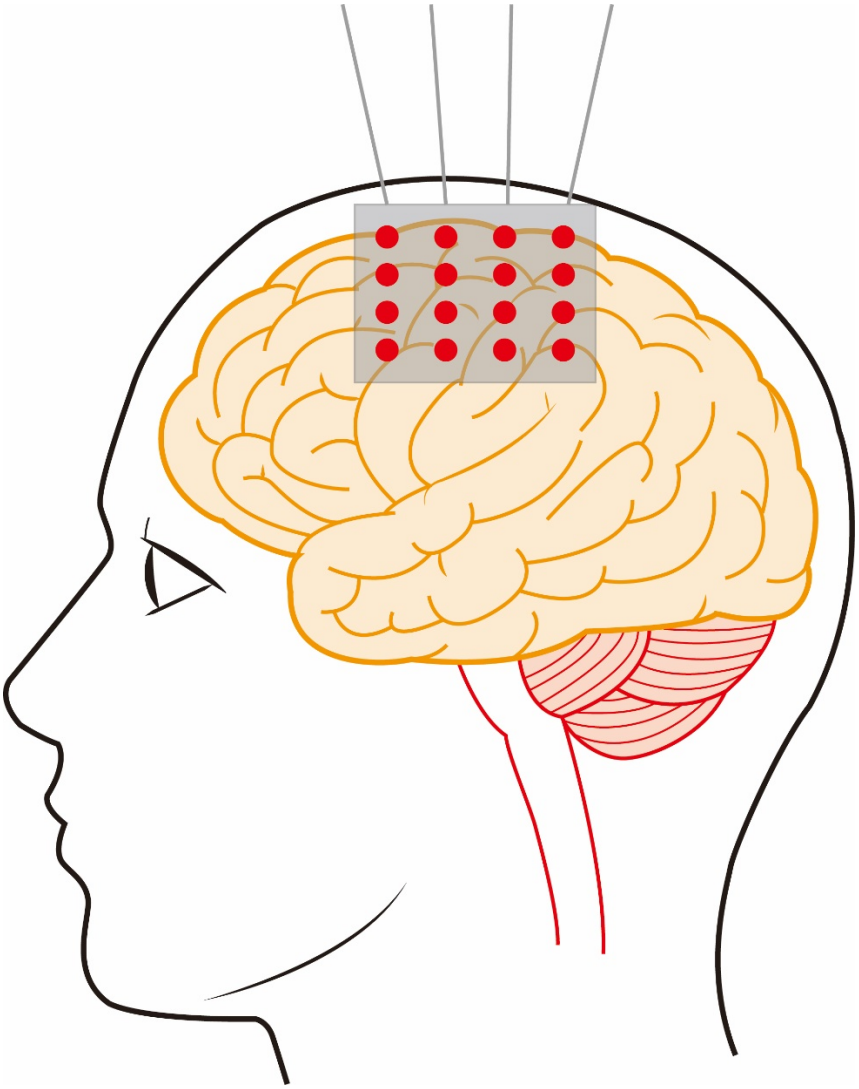

Figure 1.2: Electrode array for ECoG measurement.

Non-invasive BMI system uses neural signals, such as electroencephalography (EEG), magnetoencephalography (MEG), functional near-infrared spectroscopy (fNIRS; Naseer and Hong, 2015; Hong and Zafar, 2018), and functional magnetic resonance imaging (fMRI), that are measured along the scalp or outside the scalp and they do not require surgery.

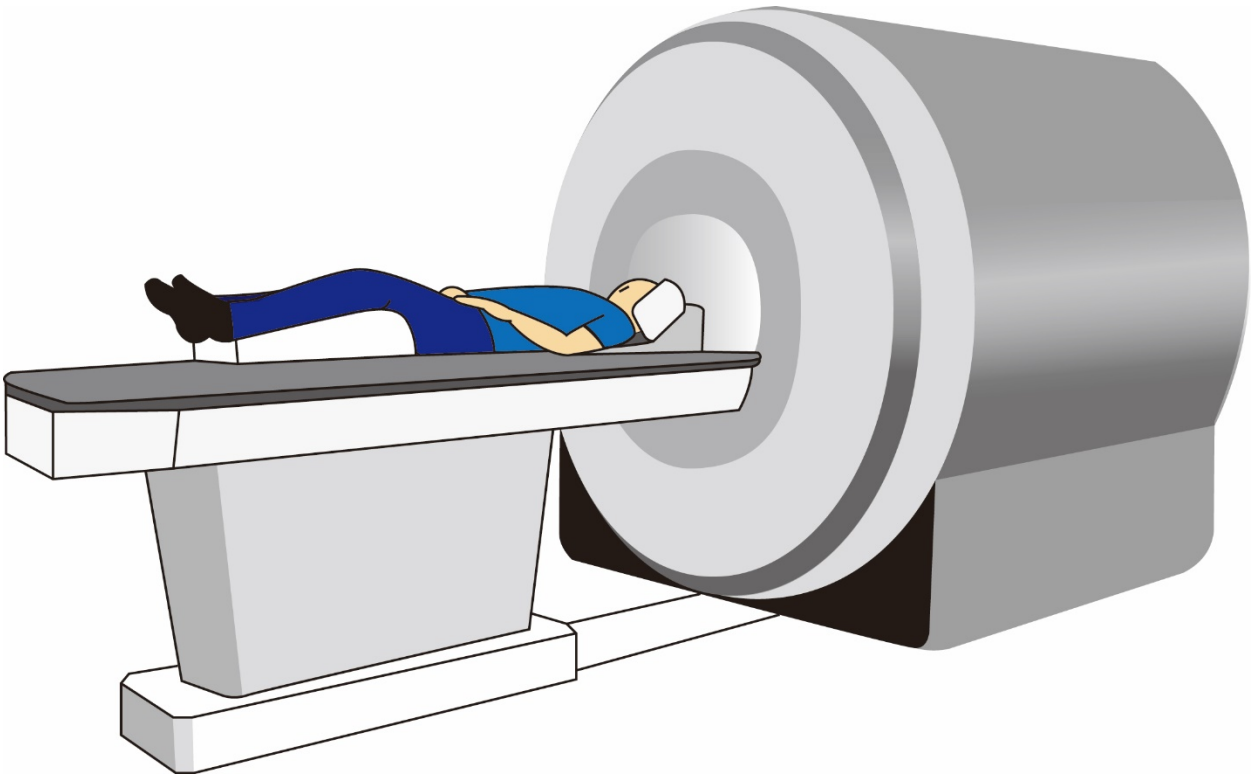

Figure 1.3: fMRI measurement.

fMRI detects the activation of the brain with blood flow. When neurons are activated, that brain activation requires blood to obtain more oxygen. Then, the amount of oxyhemoglobin increases in the activated brain area. It leads to a change in the ratio of blood with oxyhemoglobin to blood with deoxyhemoglobin, called blood-oxygen-level dependent (BOLD) contrast. Thus, fMRI measures BOLD contrast to detect activation in the specific brain areas. In addition, fMRI has high spatial resolution and low temporal resolution. For BMI applications, it was reported that fMRI-based BMI system was used to control a robotic arm (Lee et al., 2009). However, since subject's movement is restricted during fMRI recording as shown in Figure 1.3, fMRI has been more frequently used for typical neuroscience research than BMI applications.

Figure 1.4: fNRIS measurement.

fNIRS uses near-infrared spectroscopy to measure the oxygenation of hemoglobin. Since fNIRS measures similar physical quantity to that of fMRI, it also indirectly investigates neural activity of the brain. Unlike fMRI, fNIRS is portable and safe and inexpensive (Naseer and Hong, 2015), so it is easy to apply to a BMI system (Chaudhary et al., 2015). Figure 1.4 shows fNIRS measurement and subject's movement is not limited. In addition, fNIRS has high spatiotemporal resolution (Hong and Zafar, 2018). Thus, coupled with other methods to measure brain activity, fNIRS has been used for hybrid BMI system (Hong and Khan, 2017; Khan and Hong, 2017; Hong et al., 2018).

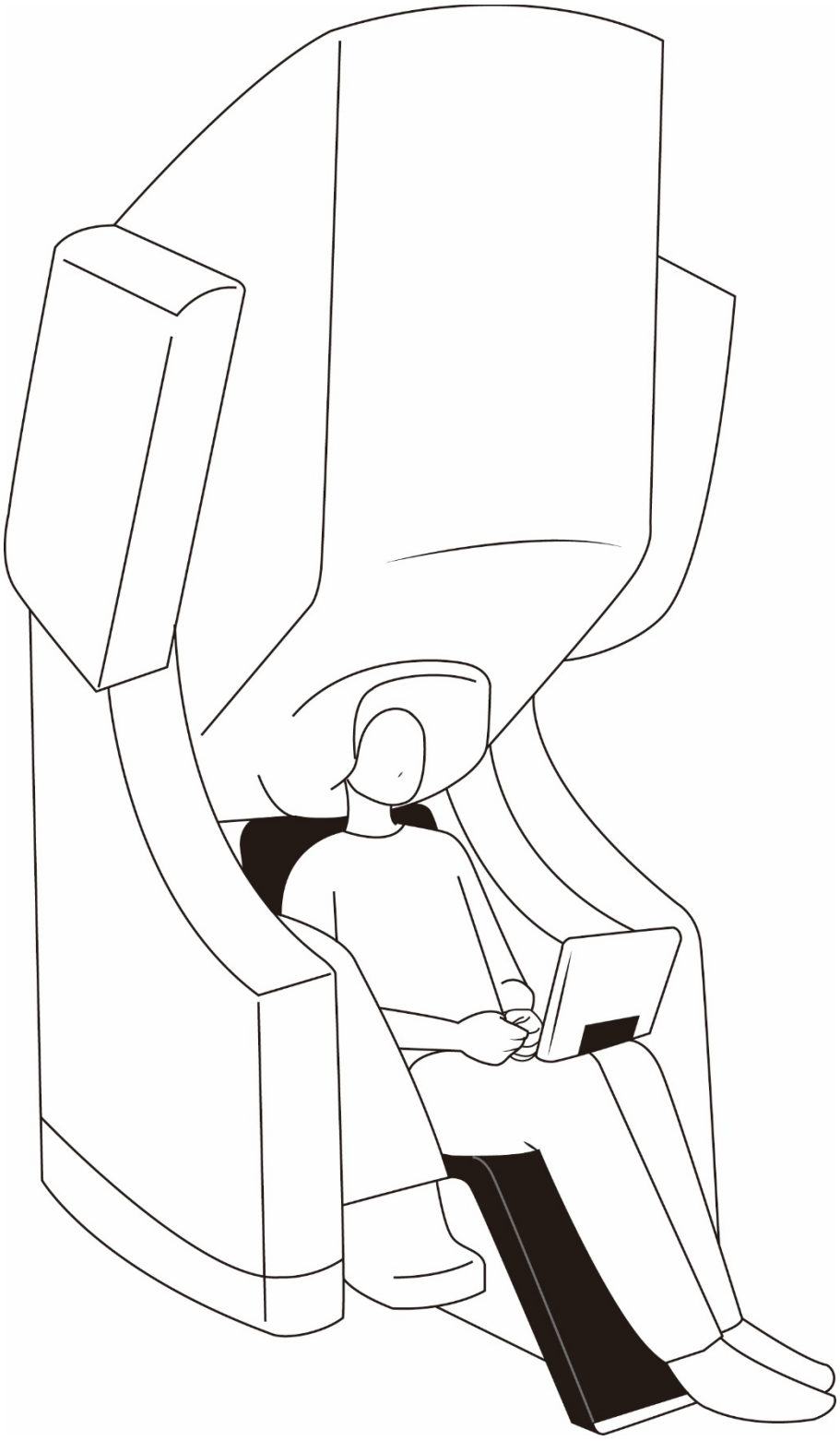

Figure 1.5: MEG measurement.

MEG measures magnetic fields from electrical currents generated by the neurons. MEG signals are measured by superconducting quantum interference device, which is a sensitive magnetometer. Unlike fMRI which detects indirect neuronal electrical activity, MEG signals reflect the direct neuronal electrical activity. MEG has better temporal resolution than fMRI. In addition, even though MEG and EEG signals reflect the same neuronal activity, unlike EEG signals, less attenuated MEG signals from current sources can be obtained because extracellular matrix may have the capacitive property (Dehghani et al., 2010). However, involved equipment is bulky as shown in Figure 1.5. Even though attempts to develop MEG-based BMI has been performed, such as development of clustering linear discriminant analysis algorithm for hand movement direction decoding (Zhang et al., 2011) and a method to process MEG-specific artifacts (Mellinger et al., 2007), similar to fMRI, MEG has been used for the purpose of typical neuroscience research rather than practical BMI research.

EEG measures the electrical activity of the brain on the scalp. EEG signals also are obtained from direct neuronal activity, so it has a high temporal resolution. Also, since EEG electrodes should be attached to each recording site one by one, EEG has a low spatial resolution. Moreover, both EEG and MEG are not free from the inverse problem (Bradshaw et al., 2001). However, MEG and fMRI have been less used for BMI system because involved equipment is bulky. As shown in Figure 1.6, users wear EEG cap with electrodes to measure EEG and their movement is not restricted. Of course, moving artifacts may arise during movement, but it is nothing compared to fMRI. Much of the noninvasive BMI system has used EEG signals as input commands.

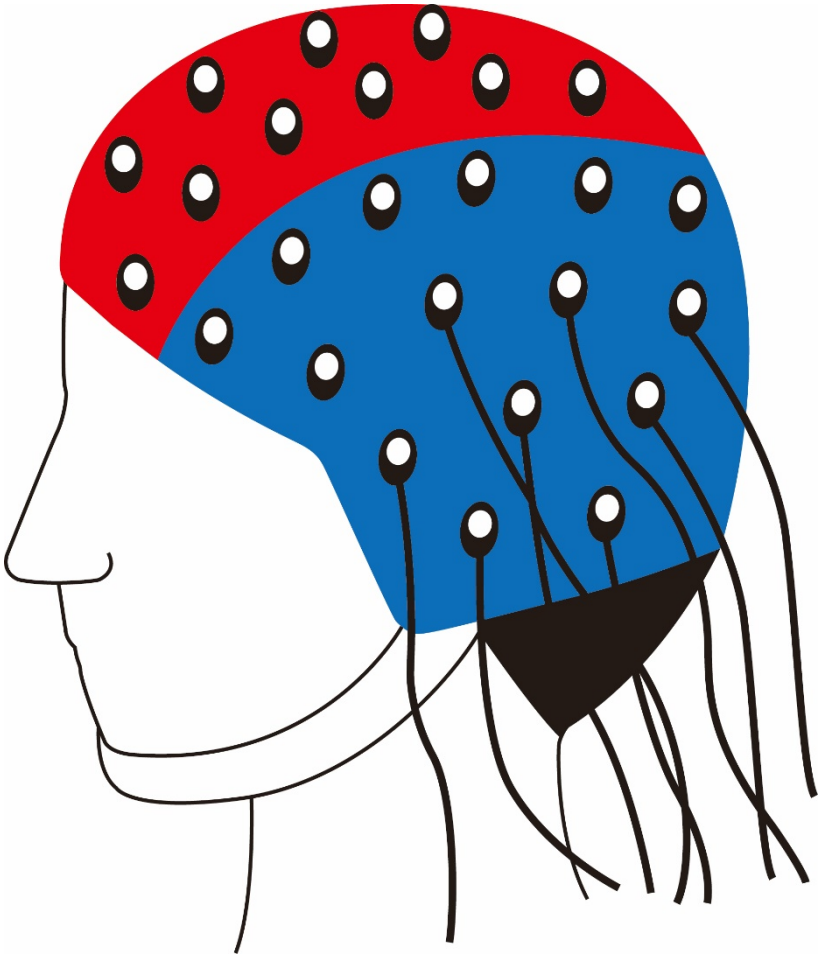

Figure 1.6: EEG measurement.

1.3 Brain activity for BMI

The central nervous system receives sensory inputs and processes them, and sends the motor output to the muscles to control them. This process is serial and different cortical areas are associated with different functions in each step. During this serial process, BMI system can use various information depending on the purpose of the system. In controlling something using BMI, it is natural and intuitive to control it as our brain controls our body. In the neuroscience field, many types of research on motor control have been performed for a long time.

It has been reported that the primary motor cortex is related to the generation of the motor command (Kakei et al., 1999). Specific areas within the primary motor correspond to different parts of the body and relatively more substantially contribute to the parts than other areas. The cortical map that illustrates the relative amounts contributing to specific parts of the body is widely known as motor homunculus (Schott, 1993). Basically, to perform a voluntary movement, sensory information is also needed because our actions interact with the world. Even though we want the same result, we have to give a different motor command to our muscles depending on both the current states of our body and the world we want to interact with. Thus, not only the primary motor cortex which directly gives a motor command but also other cortices contribute to motor control. The supplementary motor complex containing the supplementary motor area is associated with an intention to act in which neurons fire before movement execution (Nachev et al., 2008). Presupplementary motor area receives visual information and has information related to the target, while the supplementary motor area has information related to the use of the arm (Hoshi and Tanji, 2004). Also, it was reported that the dorsal premotor cortex has information related to the target in reaching movements (Cisek et al., 2003).

Many studies have been performed not only to investigate specific functions of motor-related cortices but also to explain our motor system. Our motor system can be regarded as the combined system of complex subsystems that generates motor commands suitable for our environment. Several researchers tried to explain the motor system using a model such as minimum jerk model (Flash and Hogan, 1985) and minimum torque change model (Uno et al., 1989) and to investigate characteristics of an internal model (Honda et al., 2018; Shadmehr et al., 2016).

In spite of such attempts that tried to establish an internal model, these are not enough to perfectly imitate human motor system which receives sensory inputs and generates a motor command to perform reaching movements. Thus, in BMI, motor imagery has been used as an

input command for the BMI system. When we imagine ourselves performing a specific action, our nervous system is activated as we do the action in reality. Motor imagery-based BMI systems can use imagery of various actions such as wrist extension to control upper-limb exoskeleton (Tang et al., 2016), foot movements (Hashimoto and Ushiba, 2013), and tongue movement (Pfurtscheller et al., 2006). However, upper limb imagery has been widely used, which can be measured on C3 and C4 (Tang et al., 2017; Qin et al., 2004; Ince et al., 2007; Kamousi et al., 2005). Event-related desynchronization and synchronization (ERD/ERS) were popularly used for the classification of motor imagery since ERD/ERS has been shown as a significant feature (Neuper et al., 2005), and they also have shown good performances.

1.4 Human intention in BMI

Even though motor imagery has been widely used, a motor imagery-based BMI system performs only simple few functions because it behaviors by comparing the input command with the command configuration already programmed into the BMI system and it requires the user to learn how to evoke. However, in order to construct intuitive and advanced BMI systems, the system should understand human intention. These BMI systems can be coupled with passive BMI (Zander and Kothe, 2011). Thus, various types of information have been classified to predict human intention, including that related to several types of movements performed during motor rehabilitation therapy (López-Larraz et al., 2014), different levels of ankle force (Jochumsen et al., 2013), standing and sitting (Bulea et al., 2014), the onset of voluntary movement (Ibáñez et al., 2014), mental arithmetic/rest (Naseer et al., 2016), finger movements (Liao et al., 2014), and braking intention (Kim et al., 2015).

Reaching is a fundamental and essential task in daily life. Understanding how reaching movements are represented in the brain and decoding these movements are important issues in BMI research. Several studies have attempted to decode reaching movements. For example, a

study estimated the trajectory of hand movements by applying a Kalman filter to EEG data (Robinson et al., 2015), while others decoded kinematic parameters based on EEG signals during movement (Bradberry et al., 2010; Úbeda et al., 2015, 2017). Notably, the onset of a reaching movement has been detected using EEG signals obtained 1 s prior to the onset of movement (Planelles et al., 2014).

Compared to the number of studies on brain activity during movement execution, only a few have attempted to classify the information before movement execution. Premovement brain activity has been used to detect movement intention during self-paced reaching tasks (Lew et al., 2012; Lew et al., 2014) as well as to predict targets (Novak et al., 2013), target direction (Hammon et al., 2008; Wang and Makeig, 2009), and hand kinematics (Yang et al., 2015). Moreover, studies on classification of movement direction typically used time windows that comprised target recognition after the target appeared (Hammon et al., 2008; Wang and Makeig, 2009).

After a person recognizes a target, the brain may have information regarding the target that is then processed and used to develop a motor command for reaching the target. During this planning phase, proprioception is also involved in making motor commands for reaching movements (Sarlegna and Sainburg, 2009), and information about the target and arm should be integrated prior to the movement (Hoshi and Tanji, 2000). This information may not be identical to information, such as Bereitschaftspotential (Shibasaki and Hallett, 2006), observed just prior to movement execution in a self-initiated reaching task. Several previous studies have decoded brain activity just after target appearance to predict intentions regarding reaching movements. Such studies have revealed that brain signals during target recognition can be used for decoding during reaching movement planning. For classification during movement planning, EEG data are associated with higher prediction accuracy than data acquired through other modalities such as eye tracking, electrooculography, and electromyography (Novak et al., 2013). Indeed, several studies have noted that accuracies are higher than chance level in movement direction

classification using EEG signals obtained at target appearance (Hammon et al., 2008; Wang and Makeig, 2009). For predicting peak speed and acceleration, performance is significantly better when using combined brain signals from the movement planning and execution stages than when using signals from either stage alone, suggesting that EEG signals during the planning stage can contribute to decoding (Yang et al., 2015).

1.5 Purpose of the study

The purpose of the study is to investigate brain activity during movement planning for reaching, which represents a period between target recognition and movement onset. Current many BMI systems have used brain activity during motor execution or motor imagery in which sensory input and motor command are included. Few attempts have been made at information before movement. Thus, first, we investigated the availability of EEG signals in the premovement phase. Then, we investigated which information is important for the intended reaching.

Chapter 2

Classification of Movement Intention Using Premovement EEG

2.1 Introduction

Many researchers have tried to decode brain activity to understand human motor intention from EEG signals. Linear decoding models have been used to predict upper limb kinematics during center-out reaching tasks (Úbeda et al., 2017), finger kinematics during reach to grasp movements (Agashe and Contreras-Vidal, 2011), and hand movement in three-dimensional space (Bradberry et al., 2010). However, the suitability of linear regression in modeling such tasks has been questioned (Antelis et al., 2013). Alternative modeling methods have also been applied. One study used a Kalman filter to estimate hand trajectory for a BMI (Robinson et al., 2015). Several studies on movement intention have also decoded brain activity as discrete information rather than continuous information, as in the studies cited above. Classification using discrete information has been performed for individual finger movements using a support vector machine (Liao et al., 2014), analytic movement tasks with the dominant upper limb (Ibáñez et al., 2015), as well as motor imagery for cursor control (Huang et al., 2009). Information on targets and movement direction may offer even greater versatility compared to that focusing on motor decoding. Several studies have classified movement direction (Hammon et al., 2008; Robinson et al., 2013) and targets (Shiman et al., 2017) during reaching tasks. Recently, combining EEG and fNIRS signals has been performed for early detection (Khan et al., 2018).

However, an interval before movement execution can be divided into two phases. The first phase comprises visual information. A person recognizes a target, which has information about movement direction. Then in the second phase, the person prepares to move the relevant body parts to execute movement. If the person does not wish to move immediately after target recognition, a gap may occur between target recognition and movement execution. If there is useful information for classification in this process, exploiting that information may provide improved capabilities in BMIs.

Therefore, in this chapter we investigated whether EEG signals before movement execution could be used to classify movement direction. We hypothesized that information from target recognition to movement can contribute to improvement of classification accuracy. Using independent components of EEG acquired during a premovement phase, two-class classifications were performed for left vs. right trials and top vs. bottom trials using a support vector machine. Instructions were presented visually (test) and aurally (control). In the test condition, accuracy for a single window was about 75%, and it increased to 85% in classification using two windows. In the control condition, accuracy for a single window was about 73%, and it increased to 80% in classification using two windows. Results showed that a combination of two windows from different time intervals during the premovement phase improved classification performance in the both conditions compared to a single window classification. We confirmed that EEG signals occurring during movement preparation can be used to control a BMI.

2.2 Experimental procedure

Six healthy subjects (males, mean age ± standard deviation: 27.33±1.51 years) participated in the experiment. All the subjects provided written informed consent prior to participating in the experiment. The experimental protocol was approved by the ethics committees of Tokyo Institute of Technology (Ethics number: 2015062) and was conducted in accordance with the ethical standards outlined in the Declaration of Helsinki.

Figure 2.1: Experimental environment. Subjects sat in a comfortable chair in front of a monitor on a desk with a touch pad. They adjusted their seat and the position of the touch pad to their comfort. Subjects wore a Quick-30 Dry EEG Headset (Cognionics, Inc.) to measure EEG signals. Subjects operated the touch pad with their finger.

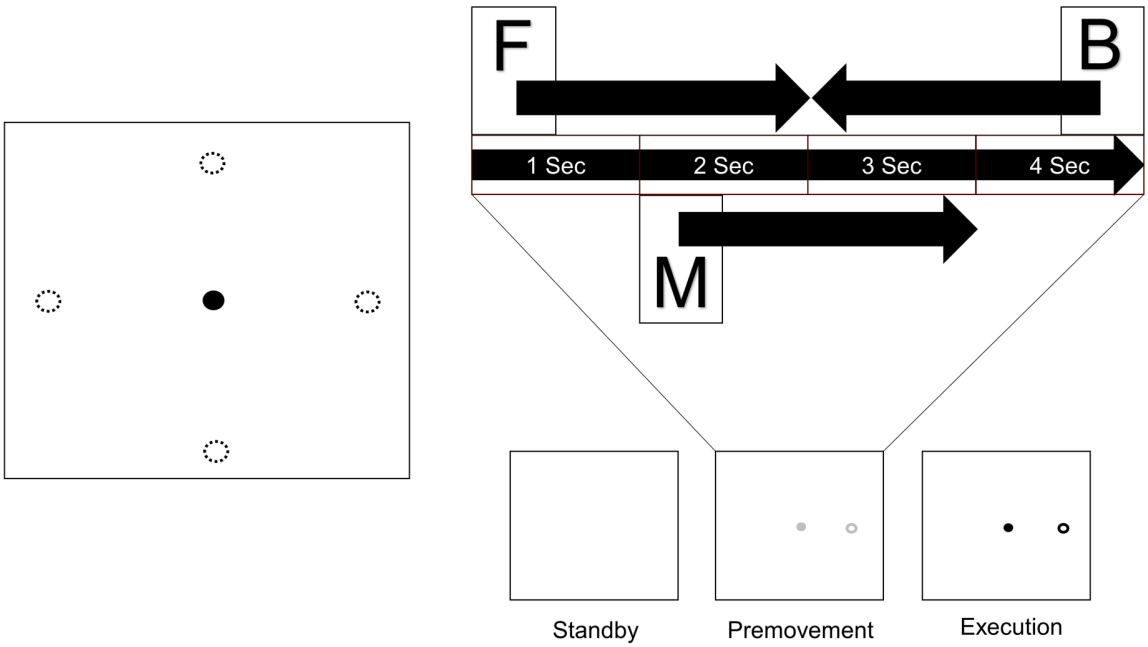

Figure 2.2: Experimental design. A target appeared at one of four positions distributed 4 cm from the center in the horizontal and vertical directions. Each trial consists of three phases. When a trial started, nothing appeared on the screen (Standby), and subjects waited for the next phase. Next, a cursor and target appeared on the screen, and subjects prepared for movement execution (Premovement). When the color of the markers changed to black, subjects moved the cursor from the center to the target using the touchpad (Execution). Three windows from the premovement phase were used for analysis (F: window starting at onset of the premovement phase, M: window starting 1 s after onset of the premovement phase, B: window before the execution phase). Four sizes were used for each window (0.5 s, 1.0 s, 1.5 s, and 2.0 s).

As shown in Figure 2.1, subjects sat in a comfortable chair in front of a monitor on a desk with a touch pad. They adjusted their seat and the position of the touch pad to their comfort. After adjustment, they placed their hand on the touch pad and waited for onset of the experiment. Figure 2.2 shows the process of a trial. One trial consisted of three phases. In the first phase (standby phase), nothing appeared on the screen, and subjects waited for the next

phase. In the second phase (premovement phase), a gray cursor and target appeared on the screen. The target appeared at one of four positions which were distributed 4 cm apart from the center in the horizontal and vertical directions. Subjects were instructed to recognize and prepare for movement execution, but not to perform it. This premovement phase lasted 4 s. In the final phase (execution phase), the color of the markers changed to black, cueing the subjects to move the cursor from the center to the target using the touchpad.

In the visual stimuli task, saccadic movements can dominantly influence classification regardless of the brain's cortical process. This is unwanted information and should be removed. We provided auditory instruction as a control condition to remove this problem. As was done in the classifications with visual instruction, classifications were performed using a single window, two windows, and spatial categorization. In the control condition, the target was invisible. When the premovement phase began, auditory instructions ("left", "right", "up" and "down") were provided. The eyes of the subjects were fixated to a cursor on the screen. When the execution phase began, a short beep sound was heard to signal the subjects to move to intended direction; and, no visual information was provided. All other procedures remained the same.

One run consisted of 40 trials, with 10 trials for each direction presented in random order. In the visual stimuli task, two of the subjects performed 5 runs, and the other four subjects performed 3 runs. In the auditory stimuli task, all of the subjects performed 5 runs. There was a rest after each run.

2.3 Data acquisition and preprocessing

EEG data were acquired from 30 electrodes (FP1, FP2, AF3, AF4, F7, F8, F3, FZ, F4, FC5, FC6, T7, T8, C3, Cz, C4, CP5, CP6, P7, P8, P3, PZ, P4, PO7, PO8, PO3, PO4, O1, O2, A2) using a Quick-30 Dry EEG Headset (Cognionics, Inc.) designed according to the international 10-20

system (Klem et al., 1999). A2 was used as a reference electrode and the ground was placed at FPz. The data were sampled at 500 Hz.

EEGLAB (Delorme and Makeig, 2004) was used for preprocessing. EEG signals were high-pass filtered at 1.5 Hz and low-pass filtered at 4 Hz. Because the value at each time point was used as a feature, low frequency components were extracted. Cut-off frequency for high-pass filter was set for good ICA performance (Winkler et al., 2015). Epochs were extracted from the premovement phase. Noisy channels and trials were rejected by visual inspection. After that, independent component analysis was performed using the extended Infomax algorithm (Bell and Sejnowski, 1995) in EEGLAB. Extracted independent components showing noise were rejected.

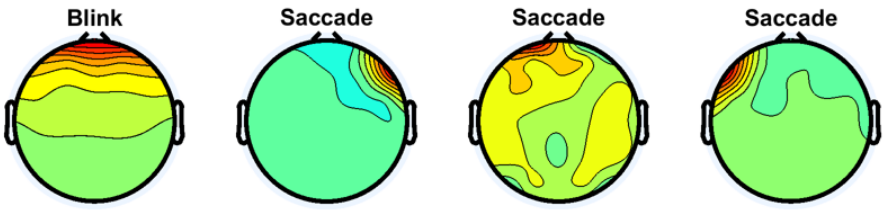

Figure 2.3: Independent components regarded as eye movement artifacts for subject 1.

Figure 2.3 shows examples of independent components regarded as eye movement artifacts for subject 1. The first independent component is a typical example of eye blinks. Similar components were observed in all subjects and rejected. The other independent components show examples of saccades. Because targets appeared leftward, rightward, upward, and downward from the center, saccades may have been included in the data. Each saccade involves

activity at either the left or right frontal site (Plöchl et al., 2012). All independent components showing such patterns were rejected for all subjects.

2.4 Classification

Independent component analysis can divide EEG signals on the scalp into multiple electrical sources (Makeig et al., 1996). We applied independent component analysis after preprocessing to find sources that could be used as features for classification. However, because the data sampled at 500 Hz offered too many features and imposed excessive computational load, the data were down-sampled to 100 Hz using EEGLAB function. Two down-sampled independent components were used for classification. Classifications were performed separately for each window using all possible pairs of remaining independent components after rejecting components. If no components were rejected, classification was performed 10,440 times for one subject.

Since the purpose of this chapter was to examine the usability of EEG signals in the interval between target appearance and movement onset, only data in the premovement phase from three time windows were used (Figure 2.2). Window F comprised visual information right after target appearance. Window M was set such that it would not include visual information. Since target recognition varies between individuals, start time of window M was set to 1s after target appearance. Window B was set such that it ended at onset of the execution phase. Each window took one of four window sizes (0.5 s, 1.0 s, 1.5 s, and 2.0 s).

Linear classifiers are widely used in BMI research (Lotte et al., 2007), and they are less vulnerable to overfitting (Muller et al., 2003). Of several linear classifiers, we employed support vector machine classifiers to perform binary classifications (left versus right and top versus bottom) because support vector machines offer strong generalization performance (Burges, 1998). Classification performance for each classifier was assessed using eight-fold cross-

validation. Classification accuracy was calculated by subtracting the percentage of the sum of misclassifications for every test set from 100%. Using the Statistics and Machine Learning Toolbox in MATLAB version 9.2.0.556344 (R2017a, The MathWorks, Inc.), support vector machine classifiers were implemented and classification performance was evaluated. Before computing classification performance, the random number generator was initialized to get the same result by applying the Mersenne Twister method (Matsumoto and Nishimura, 1998) with seed 1 (rng function in MATLAB).

Accuracies varied when using a single window for classification. Therefore, we further investigated whether combining information from different time windows would improve classification performance. Independent component pairs which provided classification accuracies greater than 65% for the single-window classifier (chance level of 50%) were used in a second classifier. Classification was performed using a total of four independent components from two windows: one pair of components from window B and another pair from either window F or window M. For each selected pair, only window sizes which provided greater than 65% accuracy were used in the classifier. For example, if only the 0.5-s window F for a pair of first and second independent components gave a classification accuracy higher than 65%, pairs from the 1-s, 1.5-s, and 2-s windows F were not considered. As was done in classification using a single window, linear support vector machine classifiers were trained using all possible combinations of independent components from two windows. Evaluation of classification performance and all other procedures remained the same.

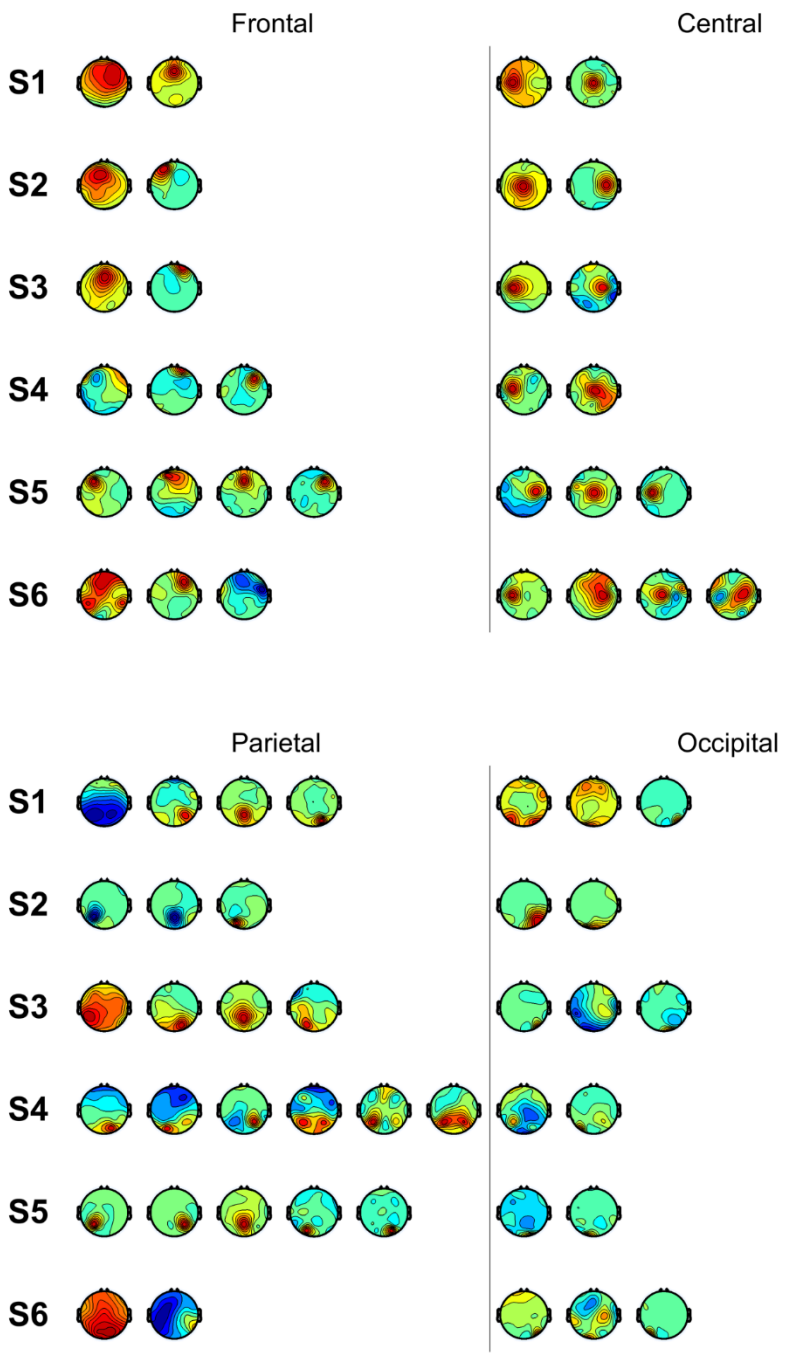

Figure 2.4: Scalp maps of independent components categorized according to area of peak activity for all subjects.

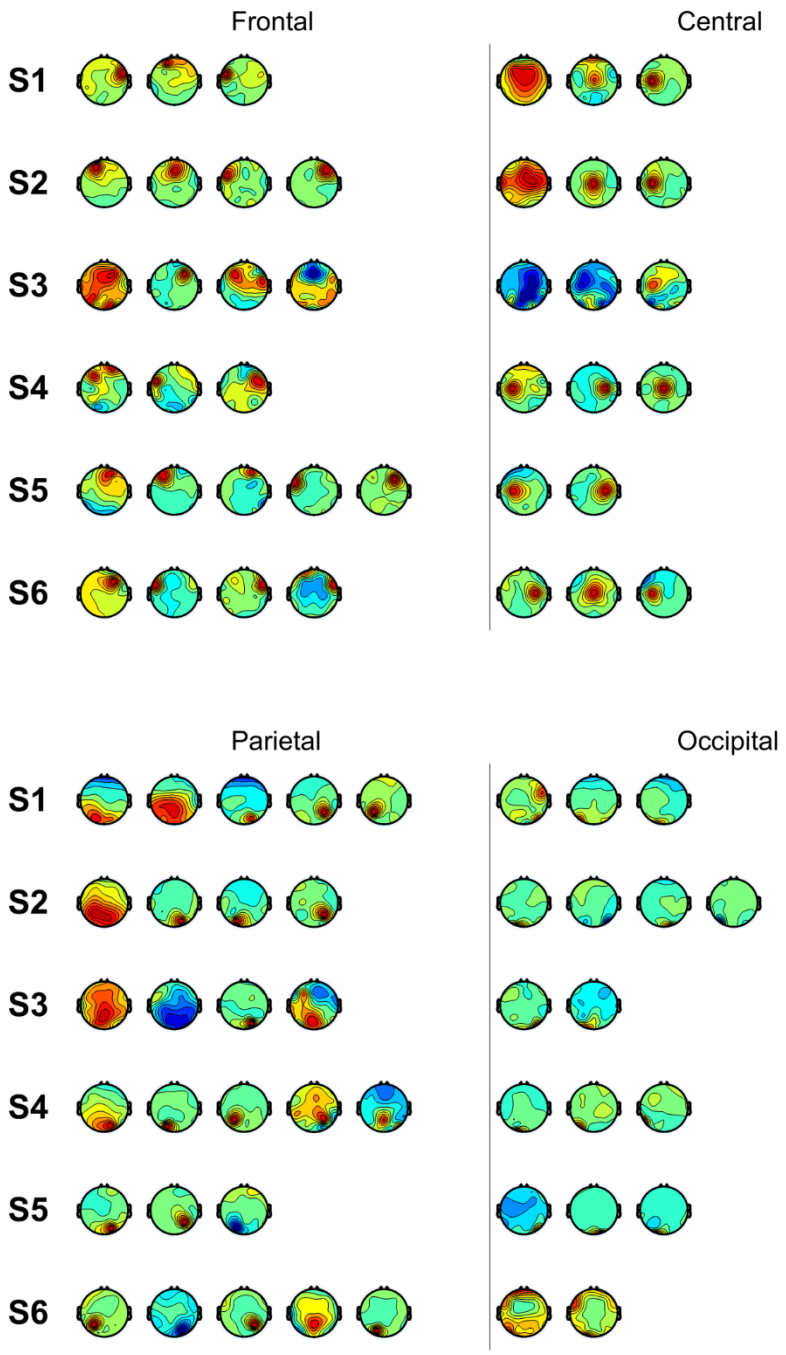

Figure 2.5: Scalp maps of independent components categorized according to area of peak activity for all subjects (control).

We also performed classification using independent components with similar spatial patterns for each subject. Figure 2.4 shows scalp maps of independent components categorized into four areas of peak activity for the test condition: frontal, central, parietal, and occipital. Figure 2.5 shows scalp maps for the control condition. The number of independent components with similar patterns was not the same for all subjects. Linear support vector machine classifiers were trained for all possible combinations of two independent components for each temporal window and brain area group. Two-class classifications (left versus right and top versus bottom) were performed, and classification performances were evaluated using the same procedure as that of the other classification methods.

2.5 Results

In the case of left versus right classification using a single window, all independent components that remained after noise rejection were used. Table 2.1 shows classification accuracies for left versus right. Most classification accuracies were above 70% except for that of subject 3, window M (67.88%). The highest classification accuracy obtained was from subject 5, window B (87.25%). Mean classification accuracies were 76.46±5.58%, 73.67±3.94%, and 76.19±5.77% for windows F, M, and B, respectively. Table 2.2 shows classification accuracies for left versus right in the control condition. The lowest classification accuracy obtained was from subject 4, window B (67.09%). The highest classification accuracy obtained was from subject 6, window B (85.42%). Mean classification accuracies were 73.23±5.24%, 73.53±4.40%, 73.65±6.60% for windows F, M, and B, respectively.

Table 2.1: Classification accuracies for left versus right. Values outside parenthesis are means of the three highest classification accuracies obtained among all independent component pairs. Values in parenthesis are means of accuracies when five inputs in shuffled conditions were fed to model which made values outside parenthesis. S indicates subject.

	Window position [%]				
	F	M	B	FB	MB
S1	73.72 (45.51)	73.72 (51.15)	73.72 (54.56)	85.90 (52.38)	85.26 (53.00)
S2	81.61 (49.46)	75.86 (49.07)	77.01 (48.87)	89.66 (48.01)	88.51 (54.59)
S3	70.91 (50.74)	67.88 (50.58)	75.15 (50.27)	85.45 (48.42)	81.21 (51.35)
S4	77.08 (48.97)	77.08 (50.27)	72.92 (49.87)	84.03 (49.78)	86.81 (50.74)
S5	84.31 (49.05)	77.45 (49.61)	87.25 (47.42)	95.10 (46.28)	97.06 (51.03)
S6	71.11 (48.80)	70.00 (49.40)	71.11 (50.41)	78.33 (47.26)	76.67 (51.47)
Mean	76.46±5.58	73.67±3.94	76.19±5.77	86.41±5.63	85.92±6.93

Table 2.2: Classification accuracies for left versus right (control). Values outside parenthesis are means of the three highest classification accuracies obtained among all independent component pairs. Values in parenthesis are means of accuracies when five inputs in shuffled conditions were fed to model which made values outside parenthesis. S indicates subject.

	Window position [%]				
	F	M	B	FB	MB
S1	68.28 (50.74)	72.04 (49.73)	73.66 (51.48)	75.81 (49.37)	79.03 (50.33)
S2	71.43 (48.89)	70.37 (51.89)	75.66 (48.53)	83.07 (48.68)	81.48 (51.12)
S3	70.98 (50.47)	72.55 (50.83)	68.24 (49.17)	76.86 (51.93)	76.86 (46.67)
S4	71.79 (49.06)	70.94 (49.34)	67.09 (50.21)	73.93 (51.73)	70.94 (51.21)
S5	73.56 (48.84)	72.99 (52.57)	71.84 (50.13)	82.76 (49.14)	84.48 (48.99)
S6	83.33 (50.32)	82.29 (49.23)	85.42 (49.97)	90.63 (47.46)	92.71 (47.35)
Mean	73.23±5.24	73.53±4.40	73.65±6.60	80.51±6.21	80.92±7.37

Left versus right classification using two windows of independent component pairs (those with single-window accuracies greater than 65%) resulted in higher accuracies than those using a single window (Table 2.1). Classification accuracies for subject 6 were 78.33% and 76.67%, using windows FB and MB, respectively. Classification accuracies for the other subjects were higher than 80%. Consistent with single-window classification, the highest classification accuracy obtained was from subject 5 using window MB (97.06%). Mean classification accuracies were 86.41±5.63% and 85.92±6.93% for windows FB and MB, respectively. Accuracies for single-

window and double-window showed significant difference ($p<0.01$, paired t-test between window F and window FB; $p<0.01$, paired t-test between window B and window FB; $p<0.01$, paired t-test between window M and window MB; $p<0.01$, paired t-test between window M and window MB). In the control condition, the highest classification accuracy obtained was from subject 6 using window MB (92.71%). Mean classification accuracies were 80.51±6.21% and 80.92±7.37% for windows FB and MB, respectively. Accuracies for single-window and double-window showed significant difference ($p<0.01$, paired t-test between window F and window FB; $p<0.01$, paired t-test between window B and window FB; $p<0.05$, paired t-test between window M and window MB; $p<0.01$, paired t-test between window M and window MB). We did not find significant differences between test and control in all windows ($p>0.1$ for all cases). We shuffled conditions and extracted signals from it to apply input to models which achieved the highest classification accuracy. Values in parenthesis of Table 2.1 and 2.2 show accuracies for models using random inputs in left versus right classification. In all cases, accuracies were about 50%.

Table 2.3 shows classification accuracies for top versus bottom. As with left versus right classification, values shown for each subject are the mean of the three highest classification accuracies among those of all independent component pairs. All classification accuracies obtained were above 70%. The highest accuracy obtained was from subject 2, window F (86.21%). Mean classification accuracies were 76.78±5.12%, 75.99±4.12%, and 74.65±4.17% for windows F, M, and B, respectively. Table 2.4 shows classification accuracies for top versus bottom in the control condition. The lowest classification accuracy obtained was from subject 4, window F (67.98%). The highest classification accuracy obtained was from subject 6, window F and B (82.76%). Mean classification accuracies were 74.11±5.46%, 74.06±4.72%, 74.55±5.00% for windows F, M, and B, respectively.

Table 2.3: Classification accuracies for top versus bottom. Values outside parenthesis are means of the three highest classification accuracies obtained among all independent component pairs. Values in parenthesis are means of accuracies when five inputs in shuffled conditions were fed to model which made values outside parenthesis. S indicates subject.

	Window position [%]				
	F	M	B	FB	MB
S1	70.99 (54.00)	72.84 (46.34)	74.07 (50.33)	80.86 (54.11)	88.27 (52.55)
S2	86.21 (52.03)	83.91 (48.89)	79.31 (46.24)	93.10 (49.73)	89.66 (49.12)
S3	75.33 (50.72)	74.00 (52.42)	71.33 (51.31)	83.33 (53.19)	86.00 (52.36)
S4	74.67 (52.03)	74.67 (50.02)	72.00 (50.24)	86.67 (50.63)	82.67 (52.14)
S5	77.78 (47.31)	76.92 (49.44)	80.34 (51.89)	93.16 (49.82)	90.60 (49.65)
S6	75.69 (54.41)	73.61 (46.44)	70.83 (52.62)	81.25 (54.42)	75.69 (49.55)
Mean	76.78±5.12	75.99±4.12	74.65±4.17	86.40±5.61	85.48±5.58

Table 2.4: Classification accuracies for top versus bottom (control). Values outside parenthesis are means of the three highest classification accuracies obtained among all independent component pairs. Values in parenthesis are means of accuracies when five inputs in shuffled conditions were fed to model which made values outside parenthesis. S indicates subject.

	Window position [%]				
	F	M	B	FB	MB
S1	69.23 (48.98)	69.87 (45.88)	75.64 (49.33)	78.21 (49.07)	80.77 (49.94)
S2	72.58 (49.48)	71.51 (50.07)	69.89 (50.21)	77.42 (48.13)	77.42 (48.95)
S3	77.27 (44.44)	75.76 (47.70)	72.22 (48.43)	86.36 (49.56)	86.36 (47.88)
S4	67.98 (50.62)	69.30 (48.55)	69.74 (49.71)	70.18 (51.43)	74.12 (49.31)
S5	74.81 (50.34)	76.30 (48.11)	77.04 (50.01)	83.70 (48.41)	82.96 (48.83)
S6	82.76 (51.92)	81.61 (45.62)	82.76 (51.25)	91.95 (48.33)	93.10 (51.49)
Mean	74.11±5.46	74.06±4.72	74.55±5.00	81.30±7.66	82.46±6.73

Top versus bottom classification using two windows achieved higher accuracy than that using a single window (Table 2.3). The lowest classification accuracy obtained was from subject 6, window MB (75.69%). Classification accuracies for the other subjects were higher than 80%. Consistent with left versus right classification, the highest classification accuracy obtained was from subject 5, window FB (93.16%). Mean classification accuracies were 86.40±5.61% and 85.48±5.58% for windows FB and MB, respectively. Accuracies for single-window and double-window showed significant difference ($p<0.01$, paired t-test between window F and window FB;

$p<0.01$, paired t-test between window B and window FB; $p<0.01$, paired t-test between window M and window MB; $p<0.01$, paired t-test between window M and window MB). In the control condition, the highest classification accuracy obtained was from subject 6 using window MB (93.10%). The lowest classification accuracy obtained was from subject 4, window FB (70.18%). Mean classification accuracies were 81.30±7.66% and 82.46±6.73% for windows FB and MB, respectively. Accuracies for single-window and double-window showed significant difference ($p<0.01$, paired t-test between window F and window FB; $p<0.05$, paired t-test between window B and window FB; $p<0.01$, paired t-test between window M and window MB; $p<0.01$, paired t-test between window M and window MB). We did not find significant differences between test and control in all windows ($p>0.1$ for all cases). Values in parenthesis of Table 2.3 and 2.4 show accuracies for models using random inputs in top versus bottom classification. In all cases, accuracies were about 50%.

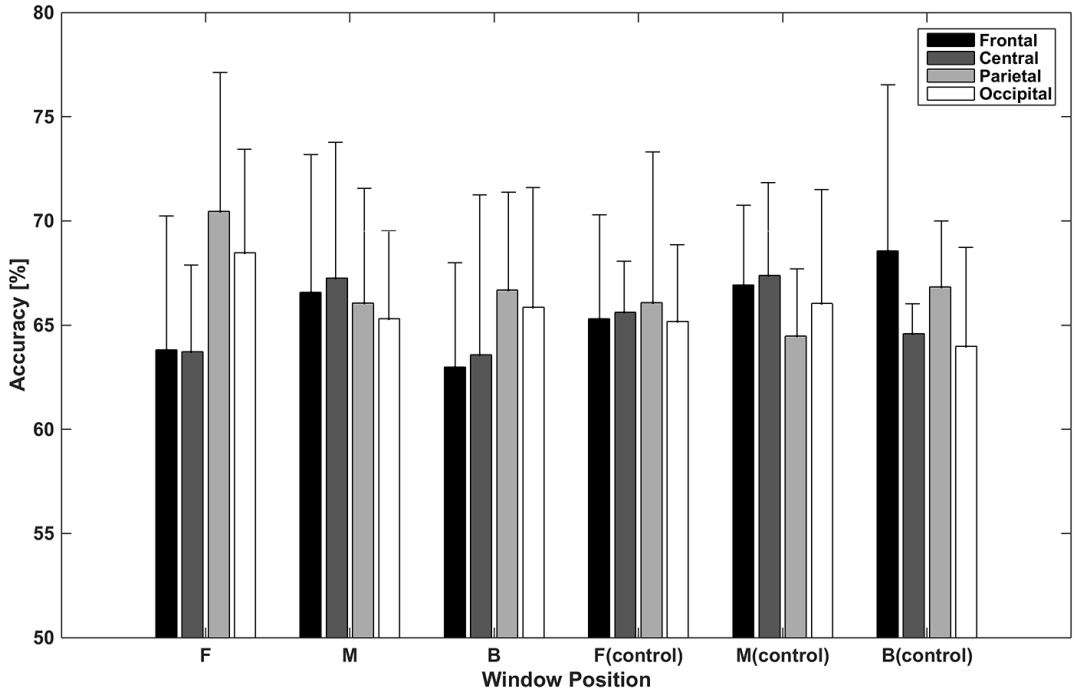

Figure 2.6: Classification accuracies using independent components categorized by spatial pattern. Values depicted are means of the highest accuracies obtained in left versus right and top versus bottom classifications averaged across subjects.

Figure 2.6 shows accuracies for classification using independent components categorized by spatial pattern. In the classifications using window F, accuracies for the parietal and occipital areas (70.46% and 68.47%, respectively) were higher than those for the frontal and central areas (63.82% and 63.72%, respectively). The difference between the former two and latter two accuracies was about 6% ($p<0.05$, t-test between the former group and latter group), while accuracies within both were less than 1% ($p>0.05$, t-test between the frontal and central area; $p>0.05$, t-test between the parietal and occipital area). In the classifications using window M, the central area provided the highest accuracy (67.26%), while the frontal area provided the lowest (65.31%); however, the difference between them was small. In the classifications using window B, parietal area achieved the highest accuracy (66.68%). The frontal area showed the lowest

performance (62.99%). In the case of the control condition, accuracies for the frontal area increased to 65.30%, 66.93%, and 68.57%. The central area showed a similar pattern in the test and control conditions. The classification using window M showed higher performance than that of window F or B. Unlike in the test condition, the difference between accuracies for the parietal and occipital areas and accuracies for the frontal and central areas was not high in window F.

2.6 Discussion

In this chapter, we investigated utilization of premovement EEG signals to classify movement direction. Previous studies on classification of premovement EEG used brain activity during phases related to visual processes (Hammon et al., 2008; Wang and Makeig, 2009). Wang and Makeig reported a mean classification accuracy of 80.25% (Wang and Makeig, 2009). In our results, accuracy using a single window was lower, at about 75%, but higher using two windows, at about 85%. Hammon et al. reported accuracies around 80% for left versus right classification and 68% for top versus bottom classification (Hammon et al., 2008). However, an exact comparison cannot be made since their experimental tasks differed from ours, with targets appearing at one of four positions distributed diagonally from the center. They also used independent components as features for classification, but they set their window after the first 500 ms. We showed that combining windows in different time phase before movement execution and using independent components for each window could improve classification performance, which suggests that optimal components may exist for each time phase. Through our results, if we found the optimal spatial area suitable for each time phase, we could improve classification performance by selecting components strategically to understand human intention. Therefore, performances in previous studies might be improved by combining information in other time phases.

Under the control condition, which could exclude the possibility of saccadic movements, the two-window classifications showed higher accuracies than those of the single-window classifications. Even when we used the windows which did not include recognition information, using both (the windows MB) showed higher accuracies compared to using either. Regardless of modalities, our result showed that combining independent components from different windows improves classification performance. In addition, we confirmed consistent performance regardless of modalities ($p>0.1$ between test and control in all windows).

In the classifications using independent components categorized according to brain area, they showed high accuracies in the control condition, unlike the components from the frontal area which showed low accuracy in the test condition. As opposed to visual instructions which are intuitive, auditory instructions require subjects to remember and translate them. It has been reported that in verbal working memory, the prefrontal cortex showed greater activation during auditory stimuli in comparison to visual stimuli (Crottaz-Herbette et al., 2004). The central area showed a similar pattern in the test and control conditions. The accuracy for window F was higher than the other windows in both conditions. The central area contributes to accuracies regardless of the modality, but the central area did not show the highest accuracies for all windows. This implies that, though there are optimal independent components for classification according to the modality, if we sacrifice some accuracy, we can use less optimal components from the central area to achieve greater generalizability. Furthermore, because the central area includes the motor cortex, which is involved in motor planning (Li et al., 2015), this trend may reflect the motor area's influence on motor preparation at each phase. The differences between accuracies for the visual stimuli and auditory stimuli were 4.38% (window F), 1.59% (window M) and -0.16% (window B) in the parietal area. The higher difference in window F may reflect that a wider parietal lobe is used to process visual stimuli compared to auditory stimuli (Poremba et al., 2003). In both conditions, the accuracies were small when the parietal area in window M was used.

However, we cannot disregard the parietal area as unessential in window M. The parietal area is involved in motor planning (Cui and Andersen, 2007) and has been used for predicting movement intention (Wang and Makeig, 2009). Desmurget et al. reported that motor intention unconsciously leads to increased parietal activity (Desmurget et al., 2009). Components from the occipital area for windows F during the test task showed the highest accuracy in both conditions. Because target recognition takes up a large portion of the early phase, it is reasonable that the occipital area, which processes visual information, would provide high performance. This trend may reflect the availability of visual information at different phases. It is useful to exploit the occipital area using an early-phase window when visual stimuli are provided.

Although we removed components related to saccadic movements, the differences between accuracies in both conditions show that the accuracy is related to the modality. It implies that the brain's activation related to stimuli can improve the accuracy. In goal directed tasks, movement is planned in the extrinsic coordinate system, but the muscle activation requires neural commands planned in the intrinsic coordinate system (Sarlegna and Sainburg, 2009). It has been reported that transformation into the intrinsic coordinate system is related to proprioception (Sober and Sabes, 2003). This physiological process could conceivably allow for decoding direction of movement even before the movement has started. However, further study is needed to determine whether the independent components used here reflect information about coordinate system transformations.

We used only EEG signals for decoding and confirmed that combining windows can improve performance. However, combining not only time phases but also other non-invasive methods can improve classification accuracy (Hong and Khan, 2017). Hybrid BMI has been studied for decoding (Hong et al., 2018) and should be studied in more detail. Therefore, features for different phases also should be investigated in hybrid BMI.

In this chapter, we confirmed that combining windows from different premovement phases offers improved performance over that using a single window. We used pairs of windows for classification. However, combining three windows, with each related to a different phase in movement preparation, may offer better performance. Because the purpose of this chapter was to investigate availability of classifiable premovement EEG, the time range was divided coarsely. Further studies that include calibration to determine optimal brain areas and time ranges could offer further progress toward a practical BMI.

2.7 Conclusion

In conclusion, we investigated whether EEG signals occurring before movement execution could be used to classify movement intention. The result showed combining windows from different time phases can improve classification accuracy rather than using single window. In addition, we found consistent performance in different modalities. Furthermore, by categorizing the independent components according to spatial pattern, we found that information depending on the modality can improve classification performance. We confirmed that EEG signals occurring during movement preparation can be used to control a BMI.

Chapter 3

Characteristics of Kinematic Parameters in Intended Reaching Movements

3.1 Introduction

Previous studies and the experiment in previous chapter have successfully shown the utility of premovement EEG for decoding during a reaching task. However, the way the brain represents information regarding the intended target during movement preparation and what information is advantageous during decoding remain unknown. Importantly, the dorsal pathway processes visual information for a reaching task. The dorsal stream carries information from the primary visual cortex in the occipital lobe to the posterior parietal lobe (Freud et al., 2016), which has visual sensory function (Hyvärinen, 1982). The information processed in this pathway might not be identical to the parameters that researchers have classified; however, the information processed by the brain is presumably related to typical classification parameters. Therefore, in this chapter, we aimed to investigate whether parameters such as direction, distance, and positions for reaching can be decoded in premovement EEG decoding.

For EEG analysis, event-related potentials (ERPs), calculated by averaging brain response epochs related to events, have been used. However, the ERP does not provide all the information about an event, and the attenuated ERP amplitude makes it difficult to analyze data in a single trial (Makeig, 1993). From a frequency viewpoint, the ERP amplitude can be regarded as power in low-frequency bands. To better utilize frequency information, EEG signals have been divided based on their amplitudes in specific frequency bands, such as alpha or beta. Event-related spectral perturbations (ERSPs) (Makeig, 1993) have also been used for EEG analysis since they represent the relative frequency spectrum amplitude in the time-frequency domain.

We extracted ERSPs using EEG independent electrical sources obtained by an independent component analysis (ICA) (Makeig et al., 1996). After selecting features for classification via analysis of variance (ANOVA), we performed all possible binary classification analyses using a support vector machine with several kinds of labeling based on movements and

movement parameters. In addition, we identified positions of the useful independent components (ICs) for classification; ICs refer to the electrical sources obtained by the ICA.

3.2 Experimental procedure

Eight individuals (6 men and 2 women, mean age ± standard deviation: 26.125 ± 3.27 years) participated in the experiment. All participants provided written informed consent prior to the experiment. The experimental protocol was approved by the ethics committees of the Tokyo Institute of Technology (ethics number: 2015062) and conducted in accordance with the ethical standards outlined in the Declaration of Helsinki.

Figure 3.1 shows the experimental environment. Each participant sat in a comfortable chair adjacent to a table. The participant wore an EEG cap and a marker for a motion sensor (Optotrak Certus, Northern Digital Inc., Waterloo, ON, Canada) was attached to the back of his/her right hand. Prior to the experiment, the participant placed his/her hand on the table to perform the required task. This position corresponded to the cursor positioned at the center of the screen. Horizontal hand movement across the table moved the cursor horizontally on the screen. However, for vertical cursor movement, the participant was required to move his/her hand vertically across the table, rather than through the air. Participants were also instructed not to touch the surface of the table during reaching movements due to the influence of friction. Thus, participants lifted their hands very slightly to perform reaching movements. The ratio between the distance of the hand and the distance of the cursor was set to 1.

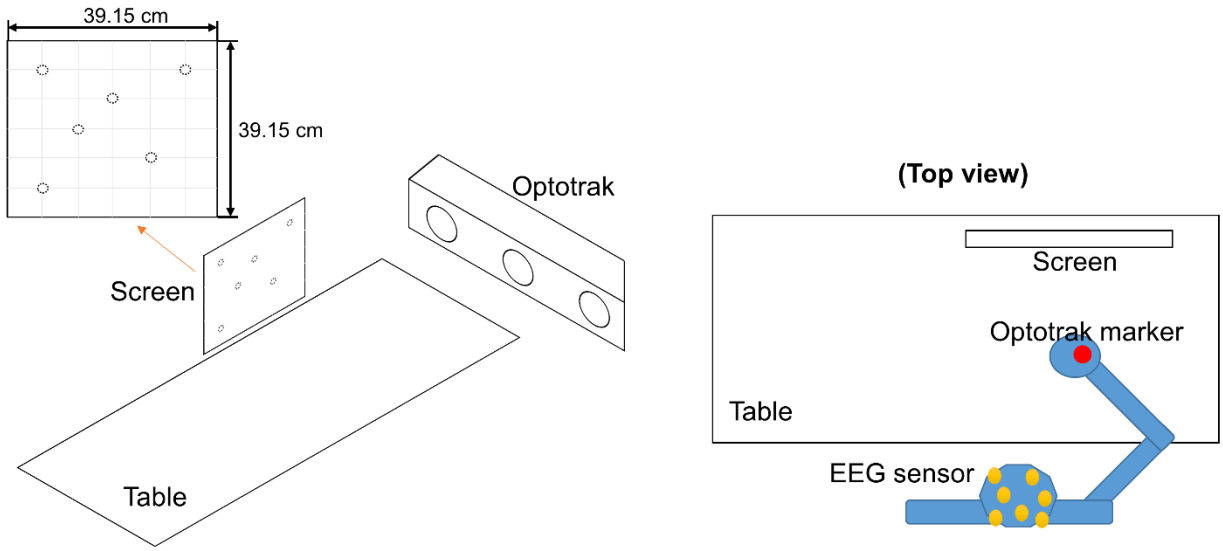

Figure 3.1: Experimental environment. The participant wore an electroencephalography (EEG) cap and sat at a desk. An Optotrak (motion sensor) marker was attached to the back of his/her right hand, and the marker position was tracked using an Optotrak device from the right side of the hand. The participant moved his/her hand on the table to move the cursor on the screen set in front of them. Horizontal movement on the table between right and left directions corresponded to horizontal movement on the screen, while vertical movement across the table between front and back directions corresponded to vertical movement on the screen. The initial cursor position and the target position were pseudo-randomly selected from the 6 positions that were decided so that all combinations from the 6 positions should cover all movement parameters (direction, distance, and positions for reaching) used in this research.

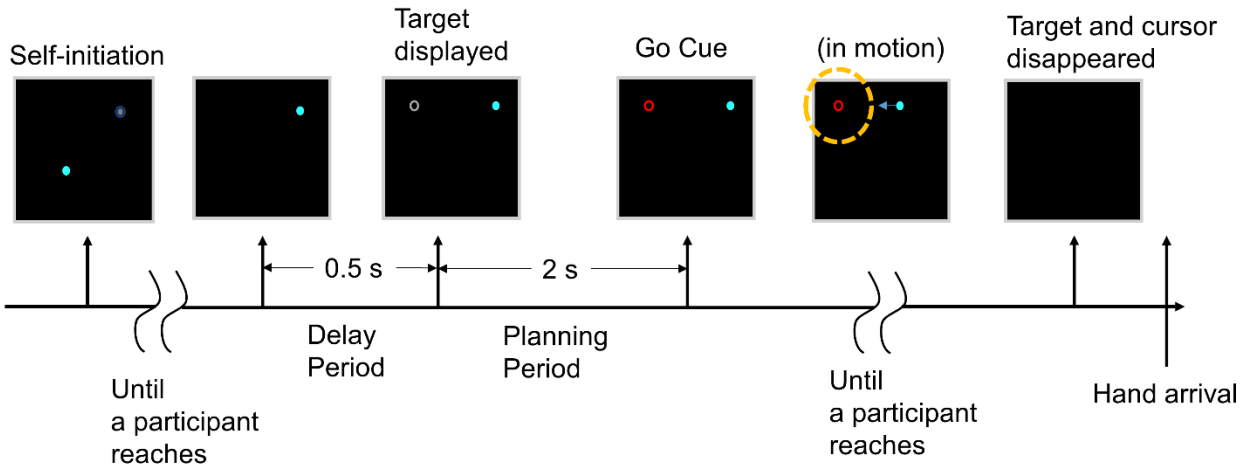

Figure 3.2: Images on the screen during a trial. At the start of the trial, an initial position indicator (a gray blurred circle) appeared at one of the 6 positions so that the participant moved the cursor (a blue circle) to the initial position by moving his/her hand. When the cursor reached the initial position, the indicator disappeared. After 0.5 seconds, a gray target appeared at one of the remaining 5 positions. The participant was instructed to prepare for movement execution for 2 seconds (planning period, premovement). When the color of the target changed to red, the participant moved his/her hand to move the cursor to the target (execution). Before the cursor completely reached the target (a yellow dotted circle in the figure), both the cursor and the target disappeared. The target and the initial cursor position were placed at 1 of 6 locations, respectively. This procedure was repeated for each trial.

Figure 3.2 shows the trial procedure. A target and the initial position of the cursor were placed at 2 of 6 locations shown in Figure 3.1. Therefore, there are 30 different movements (6 × 5 = 30) depending on the selection of the 2 positions; the 30 movements consisted of 1 of 24 directions, 7 distances, 5 target positions, respectively, as shown in Table 3.1. The participants performed the 30 different movements 10 times in 1 run. Then, all participants performed 5 runs. The trials were presented in random order, and participants were allowed to rest between runs.

Table 3.1: The 5 classes used for classification

Class				
Direction (24 classes) [Unit: degree]	Distance (7 classes) [Unit: 1 side of the small square in Figure 1: 6.525 cm]	x position (5 classes) [Unit: 1 side of the small square in Figure 1: 6.525 cm]	y position (5 classes) [Unit: 1 side of the small square in Figure 1: 6.525 cm]	Each movement
-162, -153, -146, -135, -124, -117, -108, -90, -63, -45, -27, 0, 18, 27, 34, 45, 56, 63, 72, 90, 117, 135, 153, and 180	1.414, 2.236, 3.162, 3.606, 4, 4.243, and 5.657	1, 2, 3, 4, and 5	1, 2, 3, 4, and 5	Movement 1–30

At the beginning of the experiment, an initial position indicator (a gray blurred circle) appeared to set the initial position of the cursor. The participant was allowed to take a brief break and move his/her body before moving the cursor to the initial position. When the cursor (a blue circle) reached the initial position, the indicator disappeared. After 0.5 seconds, a gray target appeared. The participant was instructed to only look at the target and prepare for movement execution in this period and not to move any body part including the eyes (planning period). During this period, the participant planned the degree and direction of movement required to reach the target. After 2 seconds, the color of the target changed to red, and the participant moved his/her hand to move the cursor to the target (execution). During this period, the

participant was instructed to reach the target in 1 attempt because feedback during movement may alter the movement trajectory (Desmurget et al., 1999). If participants were to know the final position, motor commands during the next movement may suggest an error (Tseng et al., 2007), influencing the planning phase in each trial. Therefore, before the cursor completely reached the target, both the cursor and the target disappeared. This procedure was repeated for each trial.

3.3 Data acquisition and preprocessing

Hand position was measured using the motion capture system to evaluate whether the participant moved his/her hand appropriately. The Optotrak marker was attached to the back of the hand. The position data were sampled at 100 Hz. According to the international 10-20 system (Klem et al., 1999), EEG signals were measured from the following 64 electrodes using a Biosemi Active Two amplifier system (BIOSEMI, Amsterdam, Netherlands): Fp1, Fp2, Fpz, AF3, AF4, AF7, AF8, AFz, F1, F2, F3, F4, F5, F6, F7, F8, Fz, FT7, FT8, FC1, FC2, FC3, FC4, FC5, FC6, FCz, C1, C2, C3, C4, C5, C6, Cz, T7, T8, TP7, TP8, CP1, CP2, CP3, CP4, CP5, CP6, CPz, P1, P2, P3, P4, P5, P6, P7, P8, P9, P10, Pz, PO3, PO4, PO7, PO8, POz, O1, O2, Oz, and Iz. The EEG data were sampled at 2,048 Hz.

EEGLAB (Delorme and Makeig, 2004) was used for preprocessing. The EEG signals were re-referenced to an average reference, low-pass filtered at 1 Hz, and high-pass filtered at 49 Hz. Due to the computational load, the data were down sampled to 100 Hz. Epochs were extracted from the duration between the onset of the planning period and 2 seconds post-onset (i.e., planning period). Noisy channels, noisy trials, and trials with abnormal movement as determined via visual inspection were rejected. Then, ICA was performed using the extended Infomax algorithm in EEGLAB (Bell and Sejnowski, 1995), following which noisy ICs were rejected.

3.4 Electroencephalogram analysis

Using the remaining ICs, ERSPs during the planning period were calculated using EEGLAB to identify changes in the relative spectral power for each IC with respect to the baseline. The baseline interval was defined as 200 ms before the onset of premovement to the onset of premovement (when the target appeared). The ERSP time window and the window shift sizes were 300 ms and 50 ms, respectively, in the planning period. The frequency range for ERSPs was 0–40 Hz, while the interval was 3.333 Hz. The planning period was 2,000 ms and the window size was 300 ms, so the period representing ERSP values was 1,700 ms in order not to use the period beyond the planning phase. Since the window moved every 50 ms, 34 time bins were used (1,700/50 = 34).

Figure 3.3 shows how EEG signals were processed in this chapter. We obtained 1,500 ERSPs for each time point, frequency bin, and IC. Since 1 of 30 movements was performed in each trial, a trial class could be determined according to the movement. When we classified them with direction, each trial had 1 of 24 classes because the 30 movements included 24 different directions. We assigned different classes to ERSPs, in all trials, related to the parameters because each trial had 30 movements, 24 directions, 7 distances, 5 horizontal positions, and 5 vertical positions. For each parameter, a different label was assigned to a different class. MATLAB R2019a (MathWorks, Inc., Natick, MA, USA) was used to perform an ANOVA for each parameter. The different classes comprised different groups for the ANOVA. When significant differences were observed, post hoc analyses were performed using a Tukey's honest significant difference test to identify significantly different pairs of classes. The level of statistical significance was set to 0.05. This was conducted for all ICs, time points, and frequency bins. Thus, the analyses were designed to reveal whether the ERSP of each IC at each time point and frequency bin was advantageous for the subsequent binary classification.

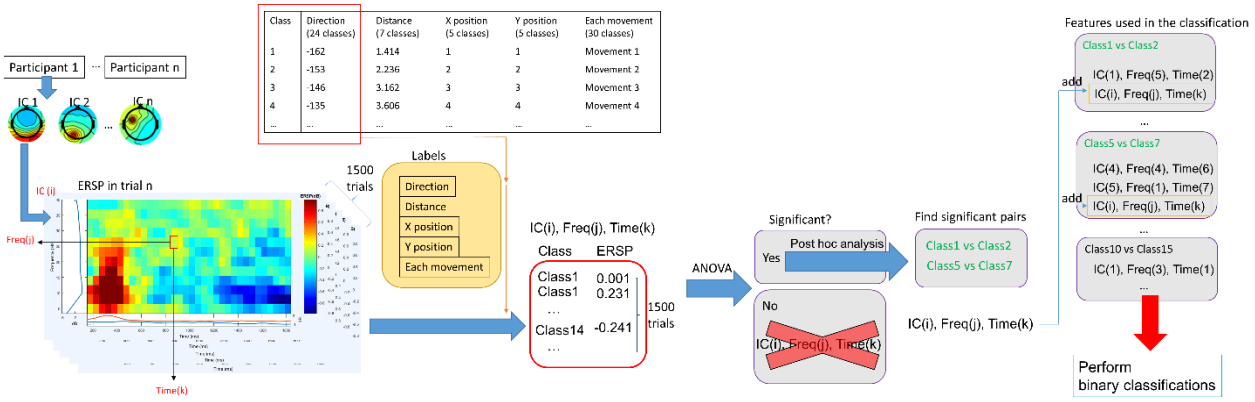

Class	Direction (24 classes)	Distance (7 classes)	X position (5 classes)	Y position (5 classes)	Each movement (30 classes)
1	-162	1.414	1	1	Movement 1
2	-153	2.236	2	2	Movement 2
3	-146	3.162	3	3	Movement 3
4	-135	3.606	4	4	Movement 4
...	...	...	...	...	...

Figure 3.3: EEG signal processing. After performing an independent component analysis (ICA), ERSPs of each independent component (IC) were calculated for each trial using EEGLAB. Then, 1,500 ERSP values were obtained at each frequency at each time point in each IC (since there were 1,500 trials). We performed classification analyses using different class labeling depending on movements (i.e., 30 movements) and parameters (i.e., 24 directions, 7 distance, and 5 horizontal and vertical positions). Then, we performed an ANOVA using the 1,500 ERSP values at each frequency at each time point in each IC. If $p > 0.05$, ERSP values at that time point at that frequency in that IC were excluded from the further analyses. If significant, post hoc analyses were performed to find significant pairs. An ERSP at a particular time and frequency in an IC was selected as a feature for subsequent binary classifications (for significant pairs). After this procedure was completed with respect to all ICs, frequencies, and times, binary classifications using significant ERSPs were performed. ANOVA, analysis of variance; Freq, frequency; ERSP, event-related spectral perturbations; EEG, electroencephalography.

Then, all possible binary classifications were performed using all significant ERSPs as features. For example, for direction classification, the binary classifications were performed 276 times (24 choose 2) per participant when the feature for all classifications had at least 1 because there were 24 different directions. When no features were extracted from the ANOVA, classification analyses could not be performed. Therefore, we assumed that each classification had at least 1 feature. A support vector machine was implemented using the Statistics and Machine Learning Toolbox in MATLAB to perform binary classifications. Classification

performance was assessed using 5-fold cross-validation. In addition, the same classifications were performed using shuffled labels to assess whether classification performance using real labels was above the chance level. The shuffled label designation was pseudorandom and balanced.

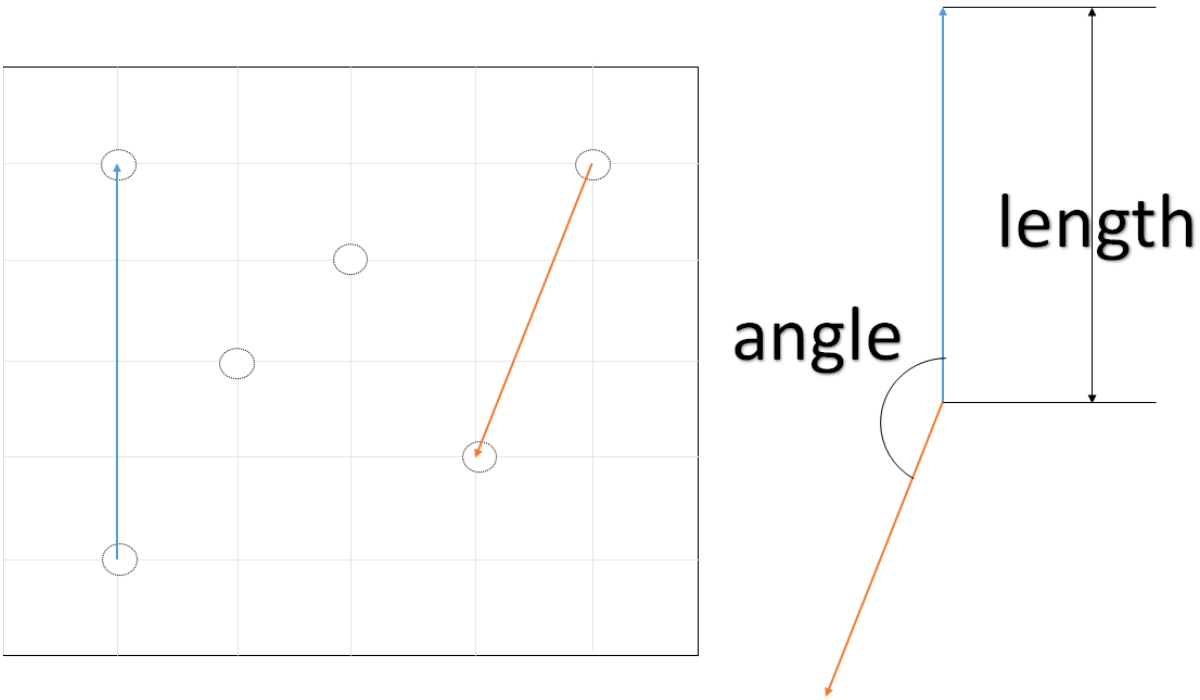

Figure 3.4: Two vectors representing different kinds of movement when each movement was used as a feature. Angle and distance of these two vectors were compared for analysis.

In contrast, for movement classifications, only 1 vector representing the movement belonged to each class and each classification always had 2 vectors to represent different kinds of movement. Thus, the parameters were investigated by comparing the 2 vectors, as shown in Figure 3.4. The following 3 values were calculated to investigate the relationship between direction and distance: angle differences, distance differences, and the sum of the distance. Since differences in the direction of the 2 vectors can have 2 values, the smaller value was selected. Regarding angle and distance differences, if accuracy for the classification where the angle

difference or distance of 2 vectors was high, 2 movements could be classified by high differences in angle or distance; this suggests that the movement may be encoded in the brain by direction or distance. The sum of the distance was calculated to investigate how this relationship changes when lengths of both vectors are too short. Positions were assessed by calculating differences in target positions. If accuracy for the classification where the differences in the distance of the 2 targets is high, the movement may be encoded in the brain by the target position.

3.5 Results

When direction and distance were used for the class, classification accuracies significantly differed between real and shuffled labels ($p < 0.01$, paired t-test). However, no such differences were observed when position was used as the class ($p > 0.1$, paired t-test); a pseudo-random balanced shuffle was used. Figure 3.5 shows classification performance when different decoding parameters were used as classes. Accuracies were averaged over the classification of all possible pairs of classes and the mean values are presented in the figure.

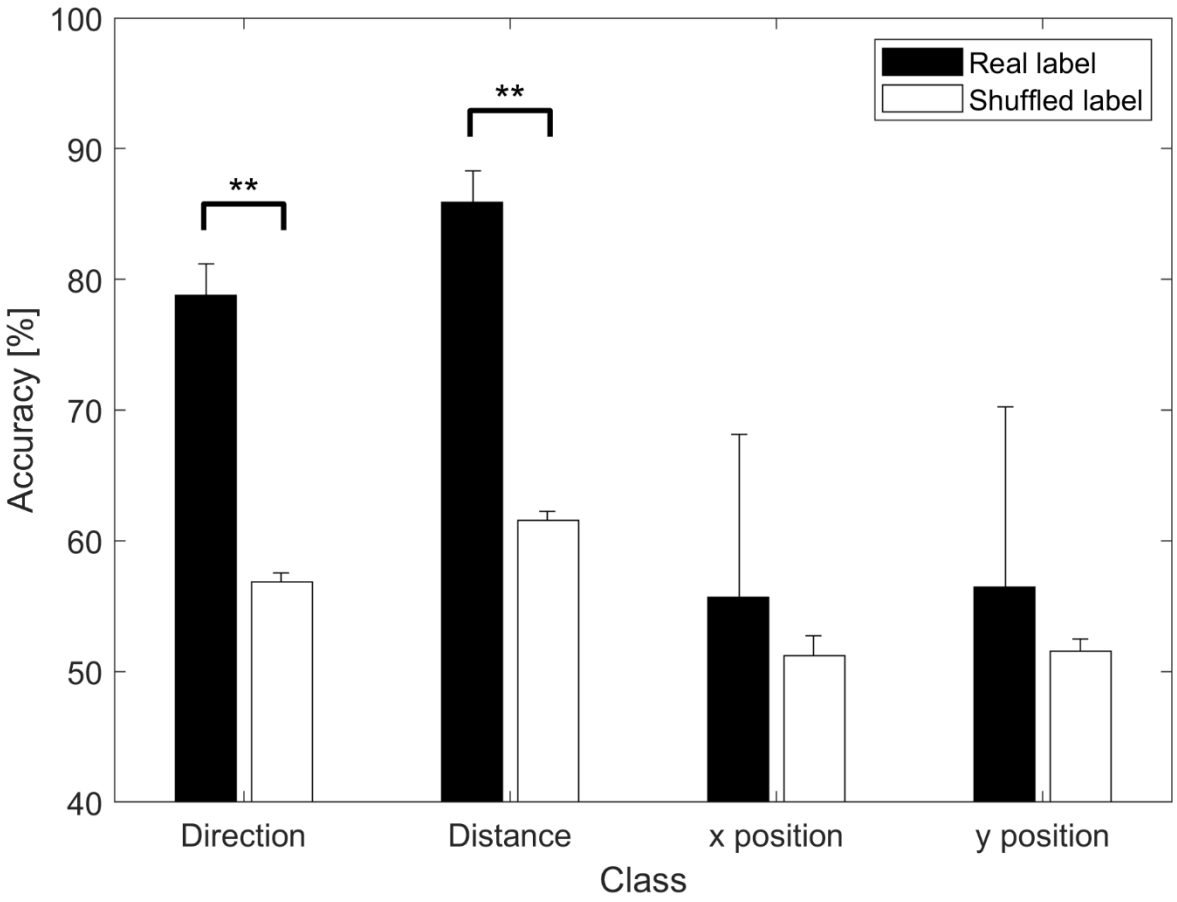

Figure 3.5: Classification accuracy based on parameters. Accuracies are represented as the means of the averaged accuracy for all possible 2-class classifications across all participants. **p < 0.01. The black bar represents the result when real labels were used while the white bar represents the result when shuffled labels were used. Significant differences were observed for direction and distance ($p < 0.01$), but not for position ($p > 0.1$).

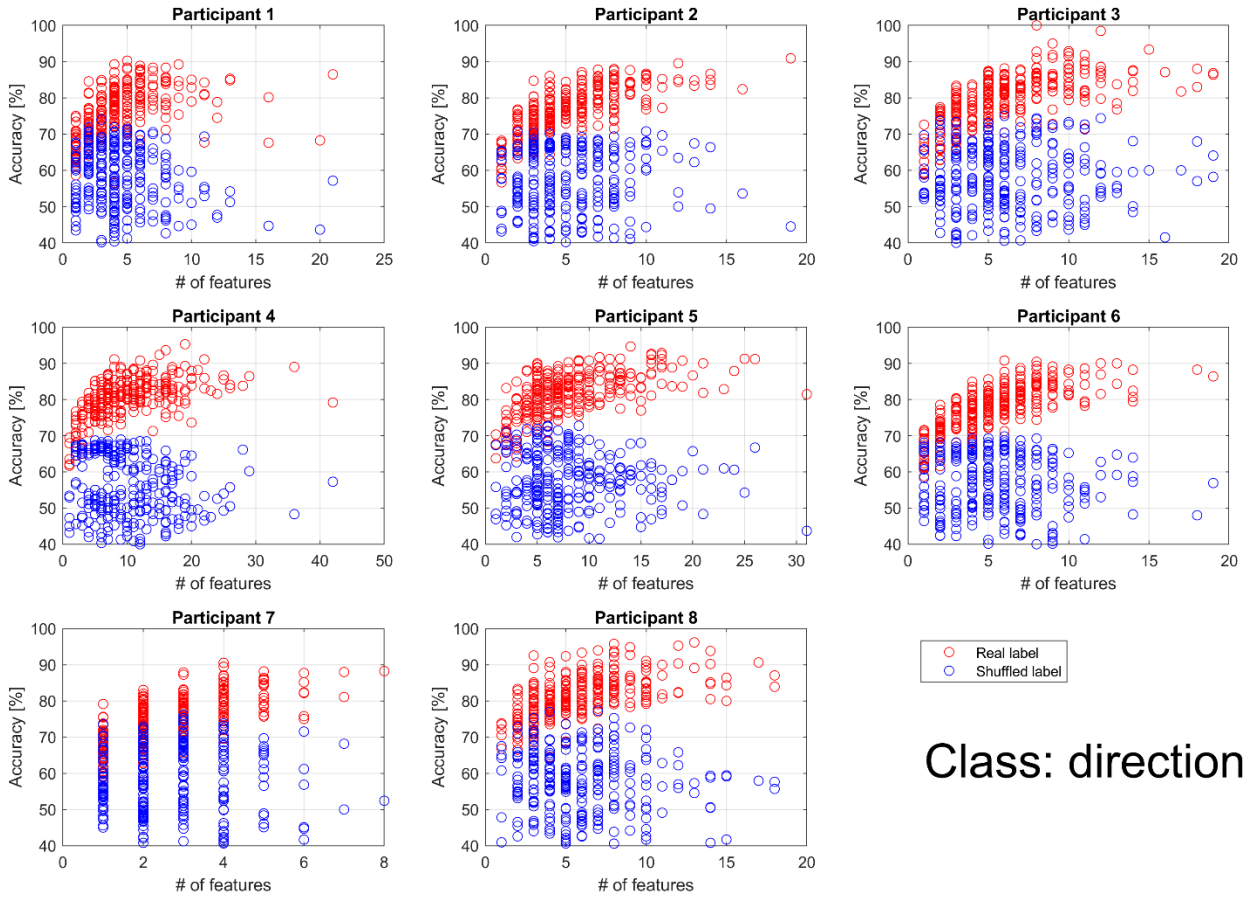

Figure 3.6: Individual classification accuracy for direction according to the number of features. Each dot represents the accuracy for each binary classification. The binary classifications were performed 276 times (24 choose 2) per participant when the feature for all classifications had at least 1. Blue circles represent the result when shuffled labels were used. Red circles represent the result when real labels were used. Performance for the real label increased in proportion to the number of features, while performance for the shuffled label did not depend on the number of features. However, performance for the real label was saturated for all participants.

For direction classification, all participants showed a higher performance than chance level. Thus, extracted features can be considered useful for the direction classification. As shown in Figure 3.6, performance for the real label increased in proportion to the number of features ($p < 0.01$ for all participants; p values were calculated for coefficients by linear regression between the number of features and the performance). For most of participants, the performance for the

shuffled label did not depend on the number of features ($p > 0.1$), while data for participant 1 and 4 showed negative significant coefficients. The performance for the real label was saturated for all participants. However, saturated accuracies for all participants were similar to each another regardless of the number of features.

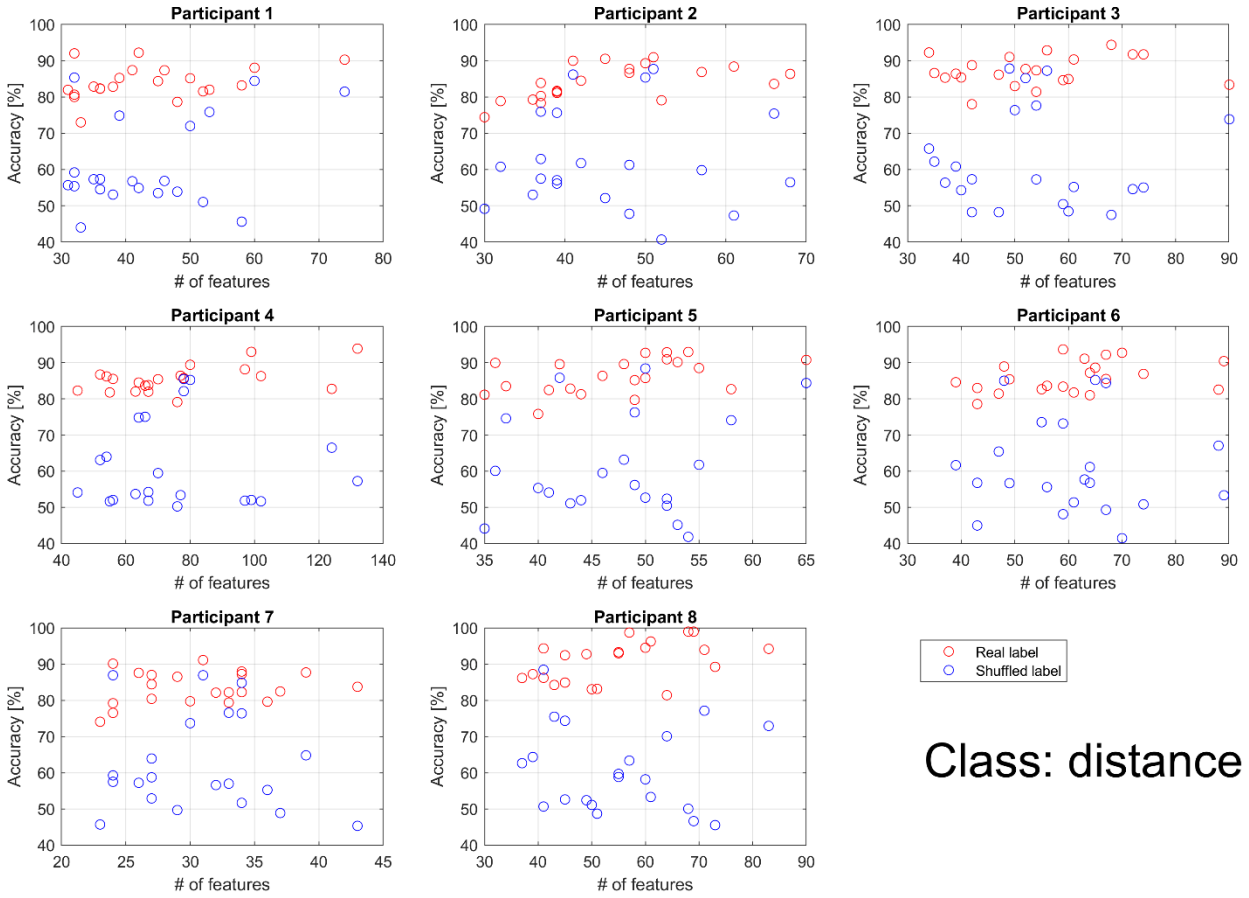

Figure 3.7: Individual classification accuracies for distance according to the number of features. Each dot represents the accuracy for each binary classification. The binary classifications were performed 21 times (7 choose 2) per participant when the feature for all classifications had at least 1. Blue circles represent the result when shuffled labels were used. Red circles represent the result when real labels were used. Performance for the real label increased in proportion to the number of features, while performance for the shuffled label did not depend on the number of features.

For distance classification, the mean accuracy was significantly higher for real labels than for shuffled labels across all participants. Thus, extracted features can be regarded as useful for the distance classification. As shown in Figure 3.7, some of participants showed that performance for the real label increased in proportion to the number of features. For real labels, data for participant 2 was statistically significant ($p < 0.01$), as well as for participants 4, 5, and 8 ($p < 0.05$). Data for the other participants showed $p > 0.1$. For shuffled labels, no participants had significant coefficients ($p > 0.1$). Unlike the direction classification, accuracy did not increase exponentially because there was no classification for which few features were utilized. In the direction classification, accuracy using shuffled labels did not exceed 80%. However, when distance was used as the class, some outliers were observed with an accuracy of more than 80%, similar to findings observed using real labels.

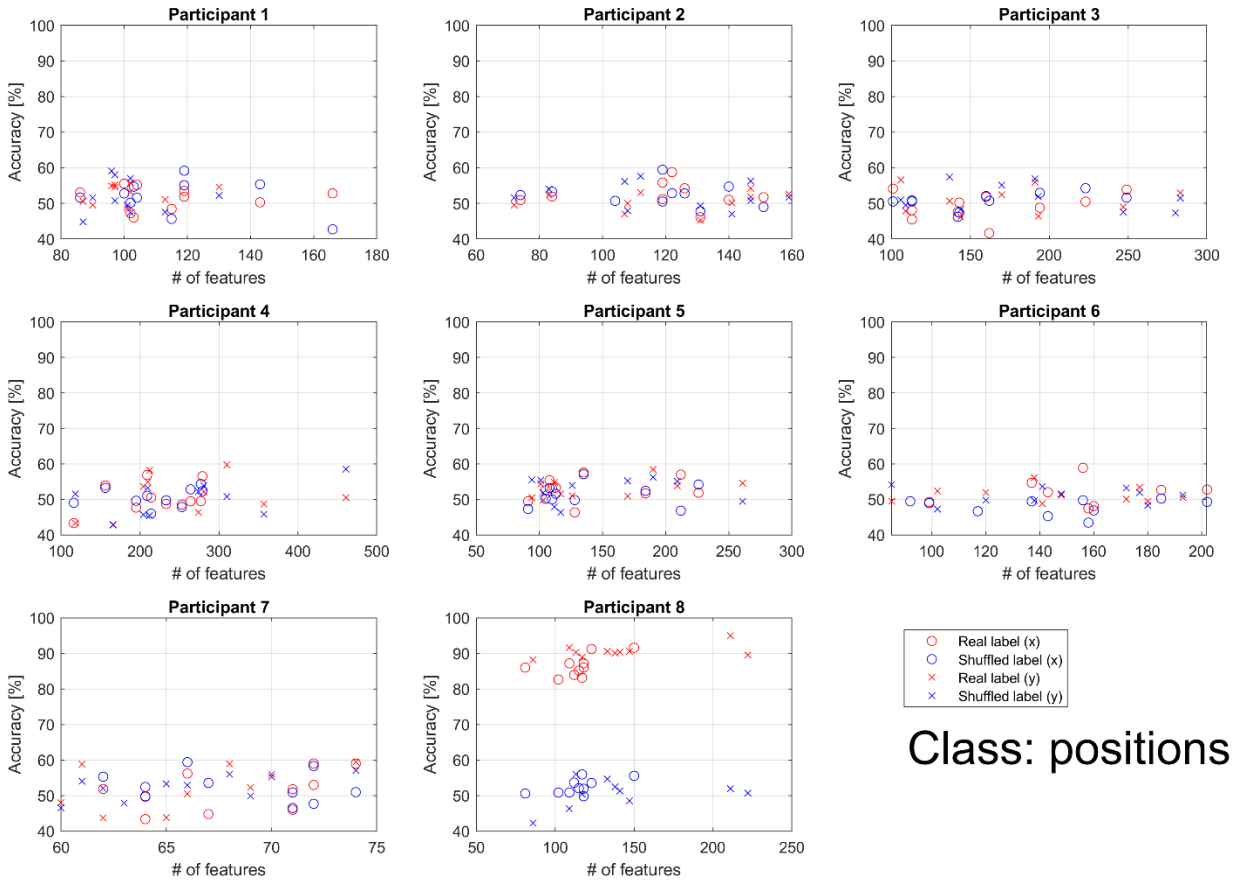

Figure 3.8: Individual classification accuracies for x and y positions according to the number of features. Each dot represents accuracy for each binary classification. The binary classifications were performed 10 times (5 choose 2) per participant when the feature for all classifications had at least 1. Blue markers represent the results when shuffled labels were used. Red markers represent the results when real labels were used. The accuracy for the horizontal (x) position is represented using circles, while that for the vertical (y) position is represented using crosses. Performance of the real and shuffled labels did not depend on the number of features. Accuracy was better than chance level in participant 8 only. For other participants, accuracy was similar to that of chance level.

For position classification, unlike the direction and distance classifications, performances for the real and shuffled labels did not depend on the number of features. As shown in Figure 3.8,

accuracy was better than chance level in participant 8 only. Accuracy was similar to that of chance level in the other participants.

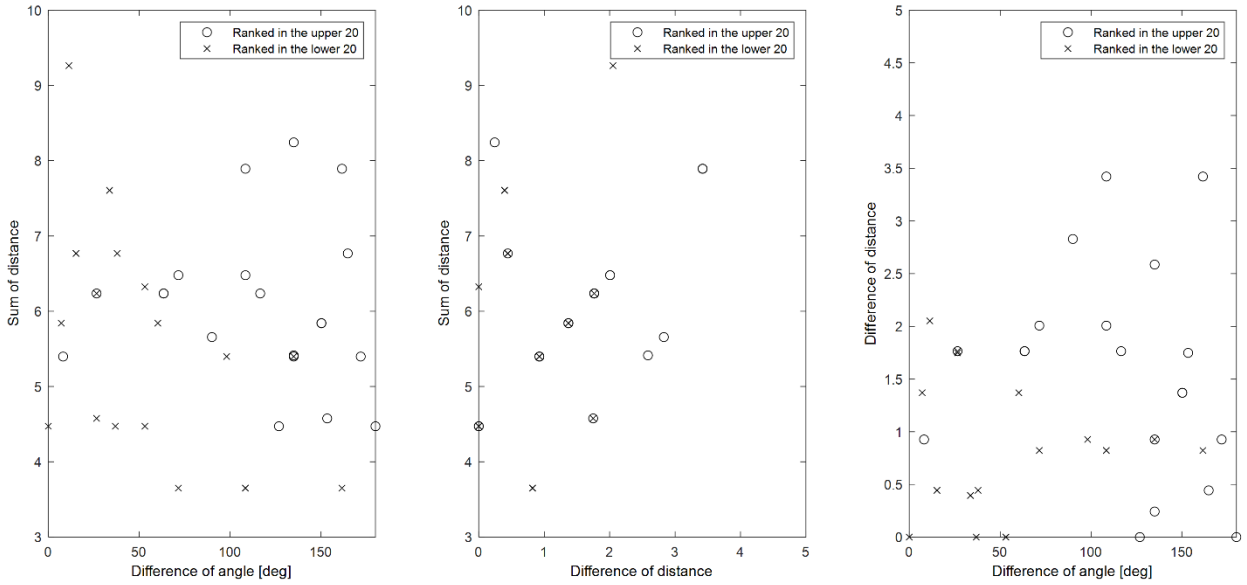

Figure 3.9: Relationships among parameters comprising 2 classes for classifications achieving high or low accuracy when all movements were used as different classes. Mean values across all participants were used for sorting accuracy. If the number of features for the individual classification was 0, the classification accuracy was not included in the mean accuracy calculation. When all movements were used as a different class, there were 435 classifications. Based on mean accuracy, circles represent the top 20 among these 435 classifications, while crosses represent the bottom 20. The angle difference, distance difference, and sum of distances comprising each vector representing the class were investigated. Since differences in the direction of the 2 vectors can have 2 values, the smaller value was selected (range: 0–180 degrees).

Consistent with findings observed in the direction classification, when each movement was used as a different class, performance for the real label increased in proportion to the number of features, while performance for the shuffled label did not depend on the number of

features. Each classification was ranked according to the mean accuracy across all participants, following which the top and bottom 20 results were selected. If the number of features for an individual classification was 0, the classification accuracy was not included in the mean accuracy calculation. Also, the relationship between direction and distance was examined. Figure 3.9 shows the relationship among parameters comprising 2 classes for the top and bottom 20 classifications. Larger angle differences and sums of distance indicate greater accuracy. Larger angle differences coupled with larger distance differences are also indicative of greater accuracy. No specific relationship was observed between the distance difference or the total distance. However, when the distance difference was more than 2, high classification performance was achieved.

For both x and y target positions when each movement was used as a different class, classification accuracy tended to be higher for greater differences in position ($p < 0.01$; ANOVA for both cases). Classification accuracy was lower for targets with low differences in position than for those with high differences in position. Figure 3.10 shows the relationship between performance and differences in target position comprising 2 classes when each movement was used as a different class. Accuracies for all 435 classifications were sorted according to mean accuracy.

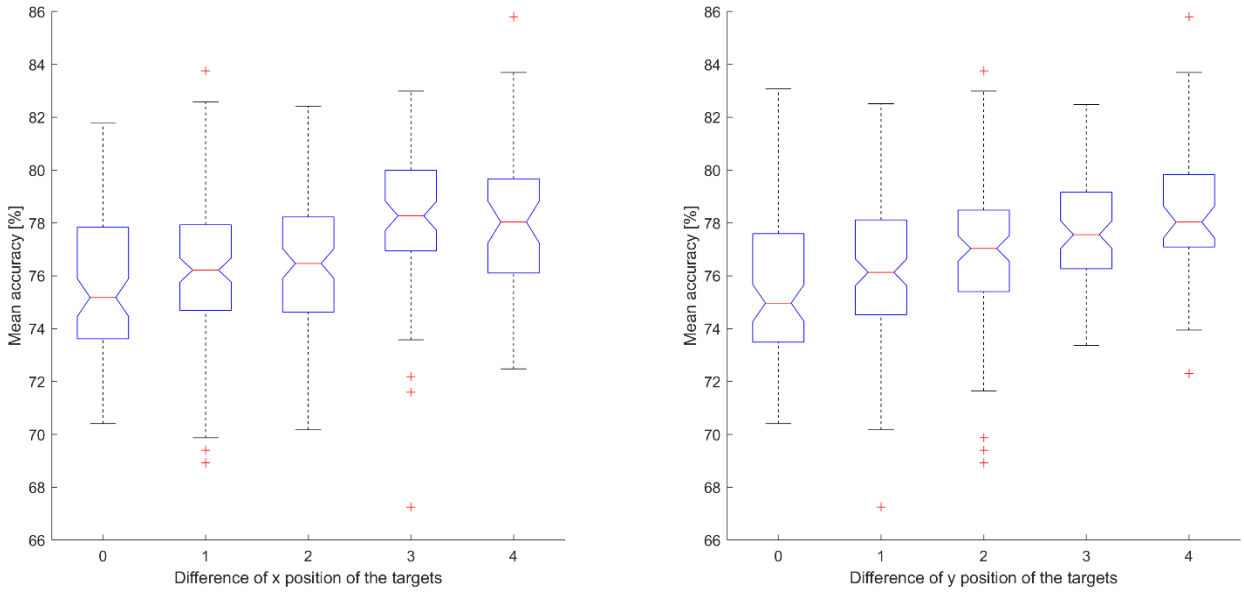

Figure 3.10: The relationship between performance and differences in the position of the target comprising 2 classes when each movement was used as a different class. Performance was calculated based on the mean accuracy across all participants. If the number of features for the individual classification was 0, the classification accuracy was not included in the mean accuracy calculation. In both cases, classification accuracy tended to be higher for greater differences in position ($p < 0.01$; ANOVA for both cases). ANOVA, analysis of variance.

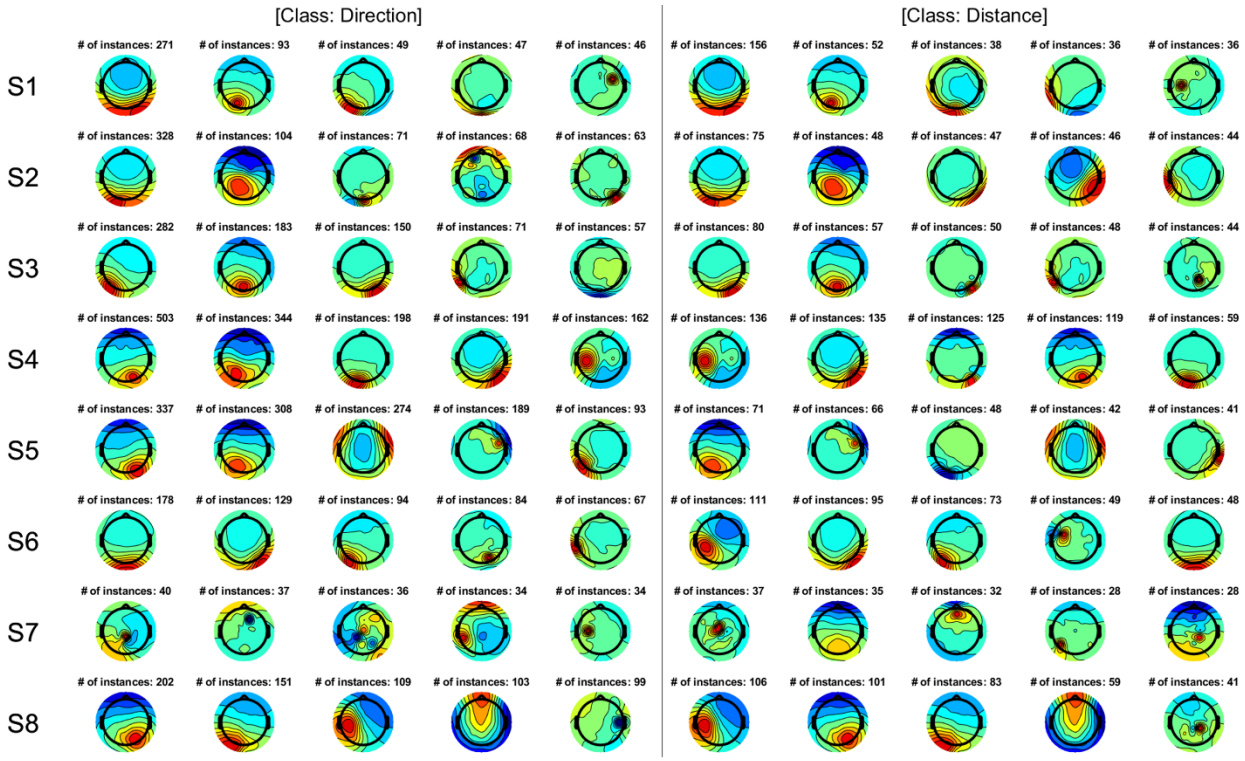

Figure 3.11: The 5 most frequently utilized ICs in all classifications for direction and distance. The number indicates the number of times the IC was used across all classifications. The ICs depicted were sorted according to the number of instances. IC, individual component.

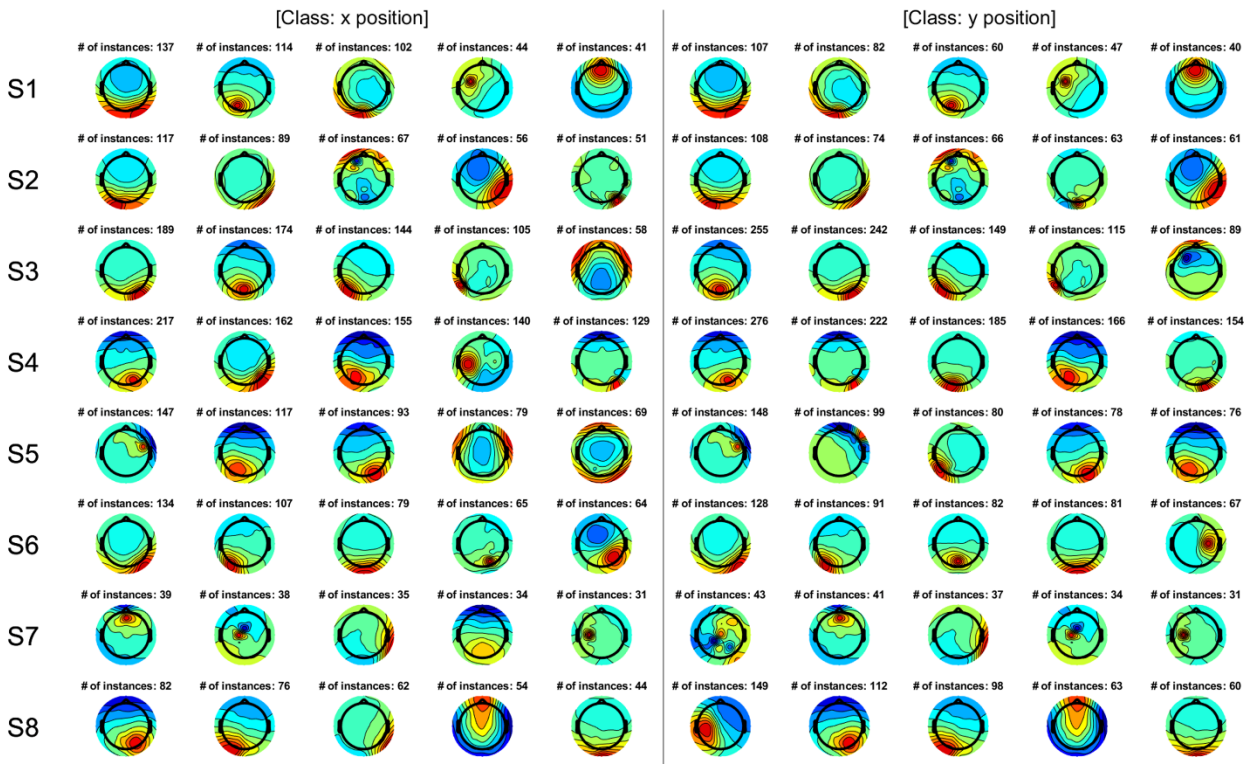

Figure 3.12: The 5 most frequently utilized ICs in all classifications for position. The number indicates the number of times the IC was used in all classifications. ICs were sorted according to the number of instances. IC, individual component.

The most frequently used ICs were investigated for classification because a relationship was observed between the number of features and classification accuracy. Figure 3.11 shows the 5 most frequently utilized ICs for all classifications for direction and distance and Figure 3.12 shows the 5 most frequently utilized ICs for classification based on position. For all parameters, ICs related to activation in the parietal and occipital areas contributed more strongly to high accuracy values than ICs related to activation in other areas and were frequently selected as significant features.

3.6 Discussion

In this chapter, we investigated the characteristics of encoded kinematic parameters of arm movement before movement execution, i.e., during movement preparation. Our analysis revealed that direction and distance classifications have some class pairs with high accuracy. Moreover, there is a relationship between these parameters (i.e., direction and distance) and the number of features extracted via the ANOVA. When each movement was used as a class, accuracy was high when the differences in the angle of the 2 vectors and total distance were high, the differences in the angle of the 2 vectors and distance were high, and the difference in the target position was high; these findings confirm that direction, distance, and position are involved in movement preparation. These observations are supported by previous findings which show the involvement of the following regions: The dorso-rostral part of Brodmann's area 5 to combine eye position and hand position to encode the target distance (Ferraina et al., 2009), posterior parietal cortex and frontal cortical areas for sensorimotor transformation during movement planning (Andersen and Cui, 2009), and parietal cortex, which integrates proprioceptive and visual information (Brunamonti et al., 2016).

In the classification for each kinematic parameter, accuracy was significantly higher than chance level for direction and distance, but not for position. However, this does not imply that information regarding target position is useless in the prediction of the intended movement, but that it is not robust because it is easily influenced by other parameters. Previous studies have reported that movement is indeed encoded based on position (van den Dobbelsteen et al., 2001; Graziano et al., 2002; Thaler and Todd, 2009).

Our results indicate that classification accuracy for direction and distance was proportional to the number of features. However, this does not mean that the number of features directly influences classification accuracy. When position was used, classification accuracy was similar to chance level regardless of the number of features. Since we used ERSPs

as a feature, a high number of features suggests that an IC showing event-related desynchronization or synchronization (ERD/ERS) in broad areas in the time-frequency domain contributes more strongly to classification accuracy than other ICs. In other words, if a feature at a specific time point or frequency bin significantly differed based on ANOVA findings but adjacent features did not, the feature may not contribute to high accuracy values. Notably, previous studies have reported ERD/ERS prior to movement execution. During the decoding of the intended movement direction, sustained ERD/ERS can be observed over the posterior parietal cortex beginning 300 ms after the directional cue (Li et al., 2012). During decoding of the intention to grasp, lift, and replace an object—which induce different kinematics—significant decreases were observed at C3 during the movement intention phase (Eilbeigi and Setarehdan, 2018). In addition, ERD has been observed at C3 prior to movement onset in the classification of different reaching movements (Shiman et al., 2017). Regions exhibiting ERD/ERS in the time-frequency domain in these previous studies exhibited values larger than each frequency bin and window shift in this experiment. As these large areas were related to decoding in previous studies, the high number of features identified in our study may also be related to decoding.

For the classification of distance using shuffled labels, some classification accuracies were high, as shown in Figure 3.7. Upon further investigation, we observed that all outliers with an accuracy of more than 70% were related to 1 class whose distance was 2.236. Only this class had 10 different directions, while the remaining classes had 2 or 4 different directions. Therefore, despite the use of shuffled labels to avoid the influence of distance, shuffled labels were classified by direction.

As shown in Figure 3.11, ICs related to activation in the parietal and occipital areas contributed more strongly to high accuracy values than ICs related to activation in other areas. The posterior parietal cortex is involved in movement preparation and intention (Snyder et al., 1997; Cui and Andersen, 2007); also, this area has been used to predict intended movement

direction in previous work (Wang and Makeig, 2009). In addition, motor intention increases activation in the parietal cortex (Desmurget et al., 2009). Moreover, the posterior parietal cortex plays a role in visuomotor transformation (Fogassi and Luppino, 2005). Such findings support the notion that the parietal area contributed to the high accuracy values observed in our study. Activation in the occipital area also likely contributed to high accuracy values, as the target was presented visually. Thus, information regarding the target should be treated as visual information that can then be used for motor planning (i.e., via the integration of somatosensory and visual information) (Sober and Sabes, 2005).

As shown in Figure 3.12, although accuracy values were similar to that of chance level, consistent with findings observed for direction and distance, ICs related to parietal and occipital activation were frequently selected as significant features. This finding suggests that position can be processed similar to direction and distance. Furthermore, the target may be coded based on both vector and position. Previous studies have reported that movements may be coded using a combination of position and vector coding (van der Graaff et al., 2014; Hudson and Landy, 2012). In accordance with these findings, our results demonstrate that parietal and occipital activation are useful for decoding.

Even when all movements were used as different classes, direction and distance were significant factors. As shown in Figure 3.9, when the distance sum (or distance difference) and angle difference are high, accuracy is also high. The figure also shows that, when 1 of these values is small, performance can be increased by increasing 1 of the other values. Thus, they complement each other, suggesting that vector coding is involved in movement. Figure 3.10 shows that greater differences in the position of the target are associated with increases in accuracy, indicating that position is also involved in movement preparation. This seems contradictory to the results presented in Figure 3.5 that indicate that there was no significant difference in accuracy relative to chance level when using real data. However, the low accuracy

values in Figure 3.5 may have been induced by various directions or distances within the class, indicating that position may not be robust for classification, and that vector coding may play a more important role than position coding. In accordance with this hypothesis, previous studies have also reported that vector coding contributes more strongly to movement than position coding (van der Graaff et al., 2014).

Participant 8 exhibited significantly high accuracy even for position decoding, as shown in Figure 3.8. Thus, for this participant, position contributed to movement preparation in a manner similar to other parameters. However, as shown in Figure 3.12, most of the top ICs were related to the parietal and occipital areas, as observed in other participants, indicating that these areas may not be related to the influence of position coding on movement representation. Further studies are required to determine whether and to what extent position coding contributes to predicting intended movement. Since the frontal area is also involved in movement planning (Andersen and Cui, 2009; Pobric and Hamilton, 2006), this area may play a different role than the parietal or occipital cortices (Connolly et al., 2007), necessitating additional studies to determine how other areas are involved in classification or decoding during movement preparation. In addition to an independent area, the contribution of multiple areas, such as the network of parietal and frontal areas, may be involved in the motor control of reaching movement (Battaglia-Mayer et al., 2014; Battaglia-Mayer and Caminiti, 2019); therefore, functional connectivity of the prefrontal cortex and dorsal premotor cortex (Mattia et al., 2010) could be considered. In participant 7, the top ICs were not related to the parietal and occipital areas as in other participants (Figures 3.11 and 3.12). However, the ICs involved achieved accuracy values similar to those observed in other participants, suggesting that other areas contribute to high accuracy. Furthermore, this finding suggests that information processed in the central area in participant 7 may be similar to that processed in the parietal/occipital area in other participants. Although future studies should aim to verify which type of information contributes most strongly to high

classification accuracy, our findings indicate that the parietal and occipital areas play a key role, and that direction and distance are advantageous for predicting intended movement.

In the current study, we calculated ERSPs of ICs at specific times and frequencies. As our approach consisted of determining significant features for each classification, this method did not reflect the fundamental differences between participant 8 and the others. Thus, an intimately linked relationship between features, including those that were not significant in this study, should be investigated. Also, connectivity between ICs should be evaluated in further studies.

3.7 Conclusion

In this chapter, we investigated the type of information the brain represents regarding the intended target during movement preparation, and what information is useful for predicting the intended movement. Our results indicated that, when each movement (i.e., pairs of the target and the initial position) was used as a labeling class, direction, distance, and position were distinguishable movement parameters for classification. However, when we classified data based on each movement parameter, only participant 8 exhibited significantly high accuracy values for the position. Thus, our findings indicate that direction and distance may contribute most strongly to the intended movement. Regardless of the parameter, our findings also demonstrate that useful features for classification are easily found over the parietal and occipital areas.

Chapter 4

Conclusion

4.1 Summary

In this study, we investigated brain activity during planning phase for reaching movement using EEG signals. Although few previous studies have shown premovement EEG signals may be used for decoding, previous studies used only part of premovement EEG signals to show the feasibility of them.

Thus, in chapter 2, we functionally separated time intervals within the planning phase and investigated whether EEG signals before movement execution could be used to classify movement direction. Our results showed that accuracies were higher than chance level regardless of the modality, inferring that brain activity during the planning phase has useful information related to the movement. In addition, a combination of two windows from different time intervals improved classification performance in the both conditions compared to a single window classification. This infers that different kinds of information related to the movement may be included in different time range within the planning phase.

Since we confirmed the availability of the premovement phase through the first experiment, in chapter 3, we tried to find what information regarding the intended target during movement preparation is advantageous for decoding. In the second experiment, we investigated whether parameters such as direction, distance, and positions for reaching can be decoded in premovement EEG decoding. In the classification for each kinematic parameter, accuracy was significantly higher than chance level for direction and distance, but accuracy for position was about chance level. Also, only participant 8 exhibited significantly high accuracy even for position decoding. For this participant, position contributed to movement preparation in a manner similar to other parameters. When all movements were used as different classes, direction and distance and position were significant factors. Thus, all parameters for this study may have information related to the movement, but the direction and the distance are more useful for predicting

intended reaching movement than the position showing significant higher accuracy for some individuals.

4.2 Future work

The parameters were not independent in our study. Our results provide useful information from a practical perspective; however, to investigate each parameter closely, an experiment should be done such that only 1 parameter varies. Especially, the direction should be more investigated closely as our results also showed good performance for the direction. It has been reported that directional tuning, which indicates preferred direction may be encoded, can be performed on some brain areas such as the primary motor cortex (Georgopoulos et al., 1982), cerebellum (Fortier et al., 1989), and Brodmann area 5 (Kalaska et al., 1983). As current sources are attenuated by many physiological factors (Buzsáki et al, 2012) to reach EEG electrodes on the scalp, if we can know how this can be reflected on EEG signals, decoding based on the neurophysiological basis can be performed. Until recently, brain activity related to the movement was decoded using EEG signals without considering or utilizing a neurophysiological phenomenon. However, recently, few studies tried to estimate sources related to directional tuning (Tanaka et al., 2018).

In addition, the brain may use other information that integrates those parameters used in our study. We recognize direction or distance, but when the brain generates motor commands, the command should be based on the muscle coordinates. When this coordinate transformation is performed within the brain remains unknown. Thus, other methods, such as estimating muscle activation using a cortical current source and classified movement direction by calculating synergy (Yoshimura et al, 2012; Yoshimura et al, 2017). Also, we can simultaneously measure muscle and brain signals to find where and when information about muscle synergy appears in the brain, so then we can better understand movement planning and how brain regions are

related to each other. Intrinsic and extrinsic coordinate movements might be identical via a synergy representation, if so, we can determine how the brain represents movement during movement planning by combining both intrinsic and extrinsic information. Therefore, how these intrinsic coordinate parameters are related to the movement planning and how they represented on EEG signals can be investigated. individuals.

4.3 General discussion

Conventional active BMI system has used neural signals such as motor imagery that can be used as input commands for the system. Figure 4.1 shows a model that describes conventional active BMI system. Neural signals are decoded to give an actuator input commands. Thus, this system performs only simple few functions and cannot prepare for a variation of an environment or human body.

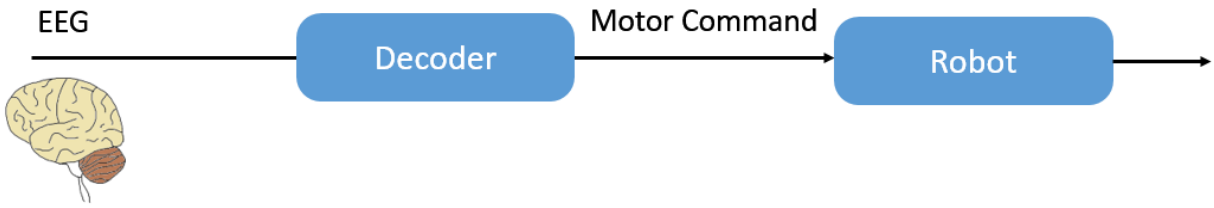

Figure 4.1: Conventional active BMI system model.

However, if we can extract useful information after movement such as reaction to delayed response of the system, it can be used for making a feedback controller to support conventional model. Then, neural signal which can be measured after movement, such as error-related potential (Schalk et al., 2000), may be used to inhibit the previous command when an error is detected or to update BMI classifiers through learning (Chavarriaga et al., 2014). Figure 4.2 shows a simple example describing combined BMI system model with a feedback controller.

Human can perceive their performance after movement, and this information can be transferred to feedback controller which can support a decoder.

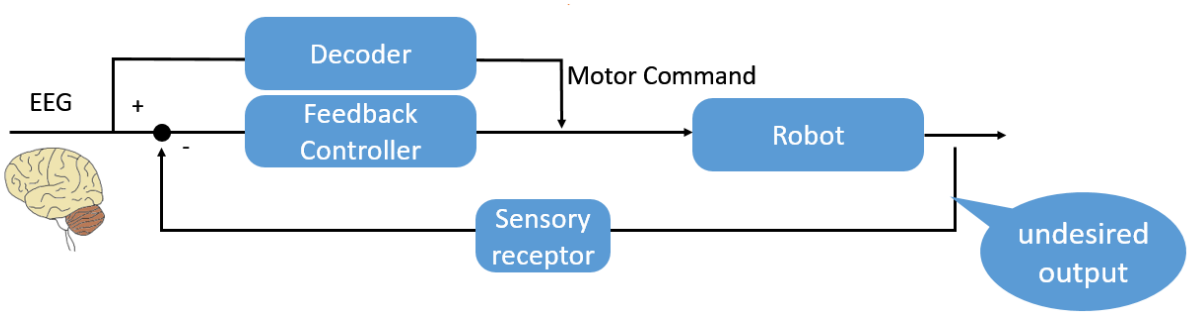

Figure 4.2: BMI system model with feedback controller.

Information not only after movement but also before movement such as information investigated in this study can be exploited. Figure 4.3 shows BMI system with feedback controller and various decoders. If we can extract useful information before movement, it can be used to decide more proper decoder suitable for current user's status or intention and to calculate the desired output in advance not to occur delay. Then, we can take a step forward to advanced and intelligent BMI system by investigating information before movement.

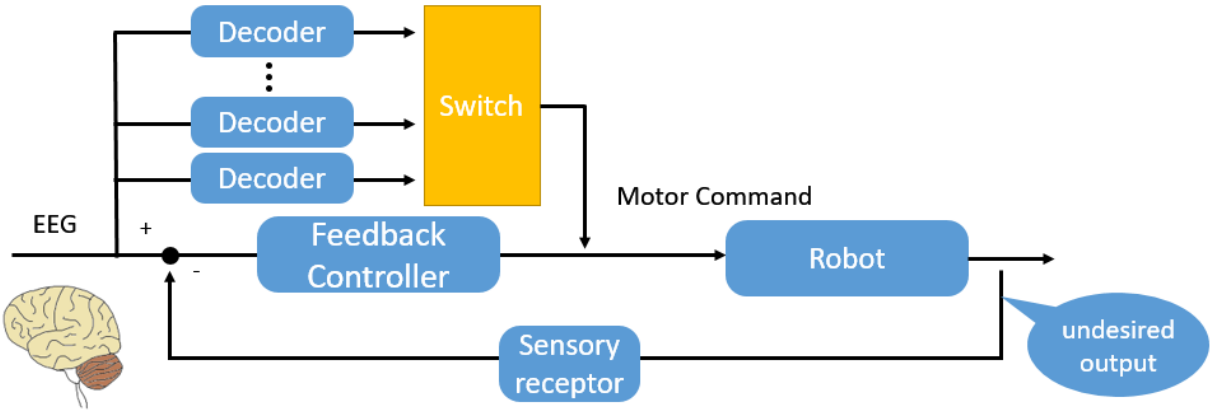

Figure 4.3: BMI system model with feedback controller and various decoders.

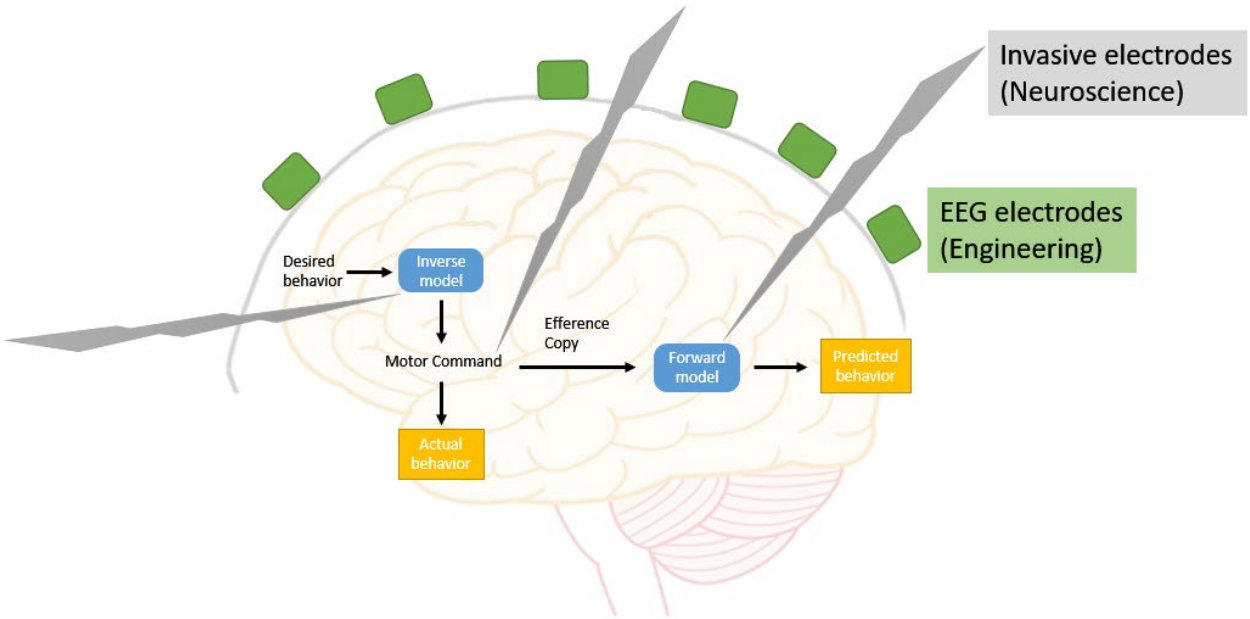

Figure 4.4: Invasive method for science and non-invasive method for engineering

In typical neuroscience field, it has been reported that kinematic parameters such as direction and distance are needed for planning by using invasive electrodes attached to monkeys. This is good for understanding specific functions in small region of the brain. For human subjects, fMRI has been used to investigate the brain. However, when we use this knowledge for practical application, EEG signals should be used because of practical reasons. Since EEG signals include combination of brain activations by many functions, it is difficult to exploit information with neurophysiological basis using EEG signals. Figure 4.4 shows invasive method that has been performed in neuroscience field to investigate specific functions and non-invasive method measuring many activations induced by many functions of the brain. Therefore, in BMI system, only simple functions have been implemented by brain activation such as motor imagery. Of course, many BMI researches have investigated information after movement and recent studies became interested in information before movement. However, in order to construct intelligent and advanced BMI system, all information, which is about movement planning, during movement

execution, and information after finishing the movement, should be used. This study showed which information is subject to be extracted easily when using EEG signals. This contributed to the field since it may help bridge the gap between neuroscience and engineering. We expect to construct intelligent and advanced BMI system exploiting all information induced by neural signals in the future.

References

Acharya, S., Fifer, M. S., Benz, H. L., Crone, N. E., and Thakor, N. V. (2010). Electrocorticographic amplitude predicts finger positions during slow grasping motions of the hand. *J. Neural. Eng.* 7(4), 046002.

Agashe, H. A., and Contreras-Vidal, J. L. (2011). ‘‘Reconstructing hand kinematics during reach to grasp movements from electroencephalographic signals,’’ *in Proceedings of the Annual International Conference of the IEEE Engineering in Medicine and Biology Society* (Bostan, MA: EMBC), 5444–5447.

Andersen, R. A., and Cui, H. (2009). Intention, action planning, and decision making in parietal-frontal circuits. *Neuron* 63, 568-583. doi: 10.1016/j.neuron.2009.08.028

Antelis, J. M., Montesano, L., Ramos-Murguialday, A., Birbaumer, N., and Minguez, J. (2013). On the usage of linear regression models to reconstruct limb kinematics from low frequency EEG signals. *PLoS One* 8, e61976. doi: 10.1371/journal.pone.0061976

Battaglia-Mayer, A., Buiatti, T., Caminiti, R., Ferraina, S., Lacquaniti, F., and Shallice, T. (2014). Correction and suppression of reaching movements in the cerebral cortex: physiological and neuropsychological aspects. *Neurosci. Biobehav. Rev.* 42, 232-251. doi: 10.1016/j.neubiorev.2014.03.002

Battaglia-Mayer, A., and Caminiti, R. (2019). Corticocortical Systems Underlying High-Order Motor Control. *J. Neurosci.* 39, 4404-4421. doi: 10.1523/JNEUROSCI.2094-18.2019

Bell, A. J., and Sejnowski, T. J. (1995). An information-maximization approach to blind separation and blind deconvolution. *Neural Comput.* 7, 1129–1159. doi: 10.1162/neco.1995.7.6.1129

Bradberry, T. J., Gentili, R. J., and Contreras-Vidal, J. L. (2010). Reconstructing three-dimensional hand movements from noninvasive electroencephalographic signals. *J. Neurosci.* 30, 3432–3437. doi: 10.1523/JNEUROSCI.6107-09.2010

Bradshaw, L. A., Wijesinghe, R. S., and Wikswo, J. P. (2001). Spatial filter approach for comparison of the forward and inverse problems of electroencephalography and magnetoencephalography. *Ann. Biomed. Eng. 29*(3), 214-226.

Brunamonti, E., Genovesio, A., Pani, P., Caminiti, R., and Ferraina, S. (2016). Reaching-related Neurons in Superior Parietal Area 5: Influence of the Target Visibility. *J. Cogn. Neurosci.* 28, 1828-1837. doi: 10.1162/jocn_a_01004

Bulea, T. C., Prasad, S., Kilicarslan, A., and Contreras-Vidal, J. L. (2014). Sitting and standing intention can be decoded from scalp EEG recorded prior to movement execution. *Front. Neurosci*. 8, 376. doi: 10.3389/fnins.2014.00376

Burges, C. J. C. (1998). A tutorial on support vector machines for pattern recognition. *Data Min. Knowl. Discov.* 2, 121–167. doi: 10.1023/A:1009715923555

Buzsáki, G., Anastassiou, C. A., and Koch, C. (2012). The origin of extracellular fields and currents--EEG, ECoG, LFP and spikes. *Nat. Rev. Neurosci.* 13(6), 407-420.

Chaudhary, U., Birbaumer, N., and Curado, M. (2015). Brain-machine interface (BMI) in paralysis. *Ann. Phys. Rehabil.* Med. 58, 9–13. doi: 10.1016/j.rehab. 2014.11.002

Chavarriaga, R., Aleksander, S., and Millán, J del R. (2014). Errare machinale est: the use of error-related potentials in brain-machine interfaces. *Front. Neurosci.* 8: 208.

Cisek, P., Crammond, D. J., and Kalaska, J. F. (2003). Neural activity in primary motor and dorsal premotor cortex in reaching tasks with the contralateral versus ipsilateral arm. *J. Neurophysiol.* 89(2), 922-942.

Connolly, J. D., Goodale, M. A., Cant, J. S., and Munoz, D. P. (2007). Effector-specific fields for motor preparation in the human frontal cortex. *Neuroimage* 34, 1209-1219. doi: 10.1016/j.neuroimage.2006.10.001

Crottaz-Herbette, S., Anagnoson, R., and Menon, V. (2004). Modality effects in verbal working memory: differential prefrontal and parietal responses to auditory and visual stimuli. *Neuroimage* 21, 340–351. doi: 10.1016/j. neuroimage.2003.09.019

Cui, H., and Andersen, R. A. (2007). Posterior parietal cortex encodes autonomously selected motor plans. *Neuron* 56, 552–559. doi: 10.1016/j. neuron.2007.09.031

Dehghani, N., Bédard, C., Cash, S. S., Halgren, E., and Destexhe, A. (2010). Comparative power spectral analysis of simultaneous elecroencephalographic and magnetoencephalographic recordings in humans suggests non-resistive extracellular media. *J. Comput. Neurosci. 29*(3), 405-421.

Delorme, A., and Makeig, S. (2004). EEGLAB: an open source toolbox for analysis of single-trial EEG dynamics including independent component analysis. *J. Neurosci. Methods* 134, 9–21. doi: 10.1016/j.jneumeth.2003.10.009

Desmurget, M., Epstein, C. M., Turner, R. S., Prablanc, C, Alexander, G. E., and Grafton, S. T. (1999). Role of the posterior parietal cortex in updating reaching movements to a visual target. *Nat. Neurosci.* 2, 563-567. doi: 10.1038/9219

Desmurget, M., Reilly, K. T., Richard, N., Szathmari, A., Mottolese, C., and Sirigu, A. (2009). Movement intention after parietal cortex stimulation in humans. *Science* 324, 811–813. doi: 10.1126/science.1169896

Eilbeigi, E., and Setarehdan, S. K. (2018). Detecting intention to execute the next movement while performing current movement from EEG using global optimal constrained ICA. *Comput. Biol. Med.* 99, 63-75. doi: 10.1016/j.compbiomed.2018.05.024

Ferraina, S., Brunamonti, E., Giusti, M. A., Costa, S., Genovesio, A., and Caminiti, R. (2009). Reaching in depth: hand position dominates over binocular eye position in the rostral superior parietal lobule. *J. Neurosci.* 29, 11461-11470. doi: 10.1523/JNEUROSCI.1305-09.2009

Fifer, M. S., Acharya, S., Benz, H. L., Mollazadeh, M., Crone, N. E., and Thakor, N. V. (2012). Toward electrocorticographic control of a dexterous upper limb prosthesis: Building brain-machine interfaces. *IEEE pulse* 3(1), 38-42.

Flash, T., and Hogan, N. (1985). The coordination of arm movements: an experimentally confirmed mathematical model*. J. Neurosci.* 5(7), 1688-1703.

Flint, R. D., Wright, Z. A., Scheid, M. R., and Slutzky, M. W. (2013). Long term, stable brain machine interface performance using local field potentials and multiunit spikes*. J. Neural. Eng.* 10(5), 056005.

Fogassi, L., and Luppino, G. (2005). Motor functions of the parietal lobe. *Curr. Opin. Neurobiol.* 15, 626-631. doi: 10.1016/j.conb.2005.10.015

Fortier, P. A., Kalaska, J. F., and Smith, A. M. (1989). Cerebellar neuronal activity related to whole-arm reaching movements in the monkey. *J. Neurophysiol.* 62(1), 198-211.

Freud, E., Plaut, D. C., and Behrmann, M. (2016). 'What' is happening in the dorsal visual pathway. *Trends. Cogn. Sci.* 20, 773-784. doi: 10.1016/j.tics.2016.08.003

Georgopoulos, A. P., Kalaska, J. F., Caminiti, R., and Massey, J. T. (1982). On the relations between the direction of two-dimensional arm movements and cell discharge in primate motor cortex. *J. of Neurosci. 2*(11), 1527-1537.

Graziano, M., Taylor, C., and Moore, T. (2002). Complex movements evoked by microstimulation of precentral cortex. *Neuron* 34, 841–851.

Hammon, P. S., Makeig, S., Poizner, H., Todorov, E., and De Sa, V. R. (2008). Predicting reaching targets from human EEG. *IEEE Signal. Process. Mag.* 25, 69–77. doi: 10.1109/msp.2008.4408443

Hashimoto, Y., and Ushiba, J. (2013). EEG-based classification of imaginary left and right foot movements using beta rebound. *Clin. Neurophysiol.* 124(11), 2153-2160.

Höhne, J., Holz, E., Staiger-Sälzer, P., Müller, K.-R., Kübler, A., and Tangermann, M. (2014). Motor imagery for severely motor-impaired patients: evidence for brain-computer interfacing as superior control solution*. PLoS One* 9, e104854. doi: 10.1371/journal.pone.0104854

Honda, T., Nagao, S., Hashimoto, Y., Ishikawa, K., Yokota, T., Mizusawa, H., and Ito, M. (2018). Tandem internal models execute motor learning in the cerebellum. *Proc. Natl. Acad. Sci. U. S. A.* 115(28), 7428-7433.

Hong, K.-S., and Khan, M. J. (2017). Hybrid brain-computer interface techniques for improved classification accuracy and increased number of commands: a review. *Front. Neurorobot.* 11: 35. doi: 10.3389/fnbot.2017.00035

Hong, K.-S., Khan, M. J., and Hong, M. J. (2018). Feature extraction and classification methods for hybrid fNIRS-EEG brain-computer interfaces. *Front. Hum. Neurosci.* 12: 246. doi: 10.3389/fnhum.2018.00246

Hong, K.-S., and Zafar, A. (2018). Existence of initial dip for BCI: an illusion or reality. *Front. Neurorobot.* 12:69. doi: 10.3389/fnbot.2018. 00069

Hoshi, E., and Tanji, J. (2000). Integration of target and body-part information in the premotor cortex when planning action. *Nature* 408, 466-470. doi: 10.1038/35044075

Hoshi, E., and Tanji, J. (2004). Differential roles of neuronal activity in the supplementary and presupplementary motor areas: from information retrieval to motor planning and execution. *J. Neurophysiol. 92*(6), 3482-3499.

Huang, D., Lin, P., Fei, D.-Y., Chen, X., and Bai, O. (2009). Decoding human motor activity from EEG single trials for a discrete two-dimensional cursor control. *J. Neural Eng.* 6:046005. doi: 10.1088/1741-2560/6/4/046005

Hudson, T. E., and Landy, M. S. (2012). Motor learning reveals the existence of multiple codes for movement planning. *J. Neurophysiol.* 108, 2708-2716. doi: 10.1152/jn.00355.2012

Hyvärinen, J. (1982). Posterior parietal lobe of the primate brain. *Physiol. Rev.* 62, 1060-1129. doi: 10.1152/physrev.1982.62.3.1060

Ibáñez, J., Serrano, J., del Castillo, M. D., Monge-Pereira, E., Molina-Rueda, F., Alguacil-Diego, I., et al. (2014). Detection of the onset of upper-limb movements based on the combined analysis of changes in the sensorimotor rhythms and slow cortical potentials. *J. Neural Eng.* 11, 056009. doi: 10.1088/1741-2560/11/5/056009

Ibáñez, J., Serrano, J. I., del Castillo, M. D., Minguez, J., and Pons, J. L. (2015). Predictive classification of self-paced upper-limb analytical movements with EEG. *Med. Biol. Eng. Comput.* 53, 1201–1210. doi: 10.1007/s11517-015- 1311-x

Ince, N. F., Tewfik, A. H., and Arica, S. (2007). Extraction subject-specific motor imagery time-frequency patterns for single trial EEG classification. *Comput. Biol. Med.* 37(4), 499-508.

Jochumsen, M., Niazi, I. K., Mrachacz-Kersting, N., Farina, D., and Dremstrup, K. (2013). Detection and classification of movement-related cortical potentials associated with task force and speed. *J. Neural Eng.* 10, 056015. doi: 10.1088/1741-2560/10/5/056015

Kakei, S., Hoffman, D. S., and Strick, P. L. (1999). Muscle and movement representations in the primary motor cortex. *Science 285*(5436), 2136-2139.

Kalaska, J. F., Caminiti, R., and Georgopoulos, A. P. (1983). Cortical mechanisms related to the direction of two-dimensional arm movements: relations in parietal area 5 and comparison with motor cortex. *Exp. Brain. Res.* 51(2), 247-260.

Kamousi, B., Liu, Z., and He, B. (2005). Classification of motor imagery tasks for brain-computer interface applications by means of two equivalent dipoles analysis. *IEEE Trans. Neural. Syst. Rehabil. Eng.* 13(2), 166-171.

Khan, M. J., Ghafoor, U., and Hong, K-S. (2018). Early detection of hemodynamic responses using EEG: a hybrid EEG-fNIRS study. *Front. Hum. Neurosci.* 12:479. doi: 10.3389/fnhum.2018.00479

Khan, M. J., and Hong, K.-S. (2017). Hybird EEG-fNIRS-based eight command decoding for BCI: application to quadcopter control. *Front. Neurorobot.* 11:6. doi: 10.3389/fnbot.2017.00006

Kim, I. H., Kim, J. W., Haufe, S., and Lee, S. W. (2015). Detection of braking intention in diverse situations during simulated driving based on EEG feature combination*. J. Neural Eng.* 12, 016001. doi: 10.1088/1741-2560/12/1/016001

Klem, G. H., Lüders, H. O., Jasper, H., and Elger, C. (1999). The ten-twenty electrode system of the International Federation. Electroencephalogr. *Clin. Neurophysiol. Suppl.* 52, 3–6.

Lee, J. H., Ryu, J., Jolesz, F. A., Cho, Z. H., and Yoo, S. S. (2009). Brain-machine interface via real-time fMRI: preliminary study on thought-controlled robotic arm. *Neurosci. Lett.* 450(1), 1-6.

Lew, E., Chavarriaga, R., Silvoni, S., and Millán Jdel, R. (2012). Detection of self-paced reaching movement intention from EEG signals. *Front. Neuroeng.* 5:13. doi: 10.3389/fneng.2012.00013

Lew, E. Y., Chavarriaga, R., Silvoni, S., and Millán Jdel, R. (2014). Single trial prediction of self-paced reaching directions from EEG signals. *Front. Neurosci.* 8, 222. doi: 10.3389/fnins.2014.00222

Li, N., Chen, T.-W., Guo, Z. V., Gerfen, C. R., and Svoboda, K. (2015). A motor cortex circuit for motor planning and movement. *Nature* 519, 51–56. doi: 10.1038/nature14178

Li, J., Wang, Y., Zhang, L., and Jung, T. P. (2012). Combining ERPs and EEG spectral features for decoding intended movement direction." *Conf. Proc. IEEE Eng. Med. Biol. Soc.* (San Diego, CA: EMBC), 1769-1772. doi: 10.1109/EMBC.2012.6346292

Liao, K., Xiao, R., Gonzalez, J., and Ding, L. (2014). Decoding individual finger movements from one hand using human EEG signals*. PLoS One* 9, e85192. doi: 10.1371/journal.pone.0085192

López-Larraz, E., Montesano, L., Gil-Agudo, Á., and Minguez, J. (2014). Continuous decoding of movement intention of upper limb self-initiated analytic movements from pre-movement EEG correlates*. J. Neuroeng. Rehabil.* 11, 153. doi: 10.1186/1743-0003-11-153

Lotte, F., Congedo, M., Lécuyer, A., Lamarche, F., and Arnaldi, B. (2007). A review of classification algorithms for EEG-based brain-computer interfaces. *J. Neural Eng.* 4, R1–R13. doi: 10.1088/1741-2560/4/2/R01

Mak, J. N., and Wolpaw, J. R. (2009). Clinical applications of brain-computer interfaces: current state and future prospects*. IEEE Rev. Biomed. Eng.* 2, 187–199. doi: 10.1109/rbme.2009.2035356

Makeig, S. (1993). Auditory event-related dynamics of the EEG spectrum and effects of exposure to tones. *Electroencephalogr. Clin. Neurophysiol.* 86, 283-293. doi: 10.1016/0013-4694(93)90110-h

Makeig, S., Bell, A. J., Jung, T.-P., and Sejnowski, T. J. (1996). ‘‘Independent component analysis of electroencephalographic data,’’ in Advances in Neural Information Processing Systems, eds D. Touretzky, M. Mozer and M. Hasselmo (Cambridge, MA: MIT Press), 145–151.

Matsumoto, M., and Nishimura, T. (1998). Mersenne twister: a 623-dimensionally equidistributed uniform pseudo-random number generator. *ACM Trans. Model. Comput. Simul.* 8, 3–30. doi: 10.1145/272991.272995

Mattia, M., Ferraina, S., and Del Giudice, P. (2010). Dissociated multi-unit activity and local field potentials: a theory inspired analysis of a motor decision task. *Neuroimage* 52, 812-823. doi: 10.1016/j.neuroimage.2010.01.063

Leuthardt, E. C., Schalk, G., Wolpaw, J. R., Ojemann, J. G., and Moran, D. W. (2004). A brain–computer interface using electrocorticographic signals in humans. *J. Neural. Eng.* 1(2), 63.

Mellinger, J., Schalk, G., Braun, C., Preissl, H., Rosenstiel, W., Birbaumer, N., and Kübler, A. (2007). An MEG-based brain-computer interface (BCI). *Neuroimage* 36(3), 581-593.

Müller, K.-R., Anderson, C. W., and Birch, G. E. (2003). Linear and nonlinear methods for brain-computer interfaces. *IEEE Trans. Neural Syst. Rehabil. Eng.* 11, 165–169. doi: 10.1109/tnsre.2003.814484

Nachev, P., Kennard, C., and Husain, M. (2008). Functional role of the supplementary and pre-supplementary motor areas. *Nat. Rev. Neurosci.* 9(11), 856.

Naseer, N., and Hong, K.-S. (2015). fNIRS-based brain-computer interfaces: a review. *Front. Hum. Neurosci.* 9:3. doi: 10.3389/fnhum.2015. 00003

Naseer, N., Qureshi, N. K., Noori. F. M., and Hong, K. S. (2016). Analysis of different classification techniques for two-class functional near-infrared spectroscopy-based brain-computer interface. *Comput. Intell. Neurosci.* 2016, 5480760. doi: 10.1155/2016/5480760

Neuper, C., Scherer, R., Reiner, M., and Pfurtscheller, G. (2005). Imagery of motor actions: Differential effects of kinesthetic and visual–motor mode of imagery in single-trial EEG. *Brain Res. Cogn. Brain Res. 25*(3), 668-677.

Novak, D., Omlin, X., Leins-Hess, R., and Riener, R. (2013). Predicting targets of human reaching motions using different sensing technologies. *IEEE Trans. Biomed. Eng.* 60, 2645–2654. doi: 10.1109/tbme.2013.2262455

Pfurtscheller, G., Brunner, C., Schlögl, A., and Da Silva, F. L. (2006). Mu rhythm (de) synchronization and EEG single-trial classification of different motor imagery tasks. *NeuroImage 31*(1), 153-159.

Planelles, D., Hortal, E., Costa, A., Ubeda, A., Iáez, E., and Azorín, J. M. (2014). Evaluating classifiers to detect arm movement intention from EEG signals. *Sensors (Basel)* 14, 18172-18186. doi: 10.3390/s141018172

Plöchl, M., Ossandón, J. P., and König, P. (2012). Combining EEG and eye tracking: identification, characterization, and correction of eye movement artifacts in electroencephalographic data. *Front. Hum. Neurosci.* 6:278. doi: 10.3389/fnhum.2012.00278

Pobric, G., and Hamilton, A. F. (2006). Action understanding requires the left inferior frontal cortex. *Curr. Biol.* 16, 524-529. doi: 10.1016/j.cub.2006.01.033

Poremba, A., Saunders, R. C., Crane, A. M., Cook, M., Sokoloff, L., and Mishkin, M. (2003). Functional mapping of the primate auditory system. *Science* 299, 568–572. doi: 10.1126/science.1078900

Qin, L., Ding, L., and He, B. (2004). Motor imagery classification by means of source analysis for brain-computer interface applications. *J. Neural. Eng.* 1(3), 135-141.

Robinson, N., Guan, C., and Vinod, A. (2015). Adaptive estimation of hand movement trajectory in an EEG based brain-computer interface system. *J. Neural Eng.* 12:066019. doi: 10.1088/1741-2560/12/6/ 066019

Robinson, N., Guan, C., Vinod, A., Ang, K. K., and Tee, K. P. (2013). Multi- class EEG classification of voluntary hand movement directions. *J. Neural Eng.* 10:056018. doi: 10.1088/1741-2560/10/5/056018

Sarlegna, F. R., and Sainburg, R. L. (2009). ‘‘The roles of vision and proprioception in the planning of reaching movements,’’ *in Progress in Motor Control. Advances in Experimental Medicine and Biology*, ed. D. Sternad (Boston: Springer), 317–335.

Schalk, G., Wolpaw, J. R., McFarland, D. J., and Pfurtscheller, G. (2000). EEG-based communication: presence of an error potential. *Clin. Neurophysiol.* 111(12), 2138-2144.

Schalk, G., and Leuthardt, E. C. (2011). Brain-computer interfaces using electrocorticographic signals. *IEEE Rev. Biomed. Eng.* 4. 140-154.

Schott, G. D. (1993). Penfield's homunculus: a note on cerebral cartography. *J. Neurol. Neurosurg. Psychiatry.* 56(4), 329.

Shadmehr, R., Huang, H. J., and Ahmed, A. A. (2016). A representation of effort in decision-making and motor control. *Curr. biol. 26*(14), 1929-1934.

Shibasaki, H., and Hallett, M. (2006). What is the Bereitschaftspotential? *Clin. Neurophysiol.* 117, 2341-2356.

Shiman, F., López-Larraz, E., Sarasola-Sanz, A., Irastorza-Landa, N., Spüler, M., Birbaumer, N., et al. (2017). Classification of different reaching movements from the same limb using EEG. *J. Neural Eng.* 14:046018. doi: 10.1088/1741- 2552/aa70d2

Snyder, L. H., Batista, A. P., and Andersen, R. A. (1997). Coding of intention in the posterior parietal cortex. *Nature* 386,167-170.

Sober, S. J., and Sabes, P. N. (2003). Multisensory integration during motor planning. *J. Neurosci.* 23, 6982–6992. doi: 10.1523/JNEUROSCI.23-18-069 82.2003

Sober, S. J., and Sabes, P.N. (2005). Flexible strategies for sensory integration during motor planning. *Nat. Neurosci.* 8, 490-497. doi: 10.1038/nn1427

Stavisky, S. D., Kao, J. C., Nuyujukian, P., Ryu, S. I., and Shenoy, K. V. (2015). A high performing brain-machine interface driven by low-frequency local field potentials alone and together with spikes. *J. Neural. Eng.* 12(3), 036009.

Tanaka, H., Miyakoshi, M., and Makeig, S. (2018). Dynamics of directional tuning and reference frames in humans: A high-density EEG study. *Sci. Rep. 8*(1), 8205.

Tang, Z., Sun, S., Zhang, S., Chen, Y., Li, C., and Chen, S. (2016). A brain-machine interface based on ERD/ERS for an upper-limb exoskeleton control. *Sensors* 16(12), 2050.

Tang, Z., Li, C., and Sun, S. (2017). Single-trial EEG classification of motor imagery using deep convolutional neural networks. *Optik-International Journal for Light and Electron Optics*. 130, 11-18.

Thaler, L., and Todd, J. T. (2009). The use of head/eye-centered, hand-centered and allocentric representations for visually guided hand movements and perceptual judgments. *Neuropsychologia* 47, 1227-1244. doi: 10.1016/j.neuropsychologia.2008.12.039

Tseng, Y., Diedrichsen, J., Krakauer, J. W., Shadmehr, R., and Bastian, A. J. (2007). Sensory prediction errors drive cerebellum-dependent adaptation of reaching. *J. Neurophysiol.* 98, 54-62.

Úbeda, A., Hortal, E., Iáñez, E., Perez-Vidal, C., and Azorín, J. M. (2015). Assessing movement factors in upper limb kinematics decoding from EEG signals. *PLoS One* 10, e0128456. doi: 10.1371/journal.pone.0128456

Úbeda, A., Azorín, J. M., Chavarriaga, R., and Millán Jdel, R. (2017). Classification of upper limb center-out reaching tasks by means of EEG-based continuous decoding techniques*. J. Neuroeng. Rehabil.* 14:9. doi: 10.1186/s12984-017- 0219-0

Uno, Y., Kawato, M., and Suzuki, R. (1989). Formation and control of optimal trajectory in human multijoint arm movement. Minimum torque-change model. *Biol. Cybern.* 61(2), 89-101.

van den Dobbelsteen, J. J., Brenner, E., and Smeets, J. B. (2001). Endpoints of arm movements to visual targets. *Exp. Brain Res.* 138, 279-287. doi: 10.1007/s002210100689

van der Graaff, M. C., Brenner, E., and Smeets, J. B. (2014). Misjudgment of direction contributes to curvature in movements toward haptically defined targets. *J. Exp. Psychol. Hum. Percept. Perform.* 40, 802-812. doi: 10.1037/a0034843.

Waldert, S. (2016). Invasive vs. Non-Invasive Neuronal Signals for Brain-Machine Interfaces: Will One Prevail? *Front. Neurosci.* 10, 295. doi: 10.3389/fnins.2016.00295

Wang, Y., and Makeig, S. (2009). ‘‘Predicting intended movement direction using EEG from human posterior parietal cortex,’’ in Foundations of Augmented Cognition. Neuroergonomics and Operational Neuroscience. FAC 2009. Lecture Notes in Computer Science, eds D. D. Schmorrow, I. V. Estabrooke and M. Grootjen (Berlin, Heidelberg: Springer), 437–446.

Winkler, I., Debener, S., Müller, K. R., and Tangermann, M. (2015). ‘‘On the influence of high-pass filtering on ICA-based artifact reduction in EEG- ERP,’’ *in Proceedings of the 37th Annual International Conference of the IEEEE ngineering in Medicine and Biology Society, (EMBC)* (Milan: IEEE), 4101–4105.

Wolpaw, J. R., Birbaumer, N., McFarland, D. J., Pfurtscheller, G., and Vaughan, T. M. (2002). Brain-computer interfaces for communication and control. *Clin. Neurophysiol.* 113, 767–791. doi: 10.1016/S1388-2457(02) 00057-3

Yang, L., Leung, H., Plank, M., Snider, J., and Poizner, H. (2015). EEG activity during movement planning encodes upcoming peak speed and acceleration and improves the accuracy in predicting hand kinematics. *IEEE J. Biomed. Health Inform.* 19, 22–28. doi: 10.1109/jbhi.2014.23 27635

Yoshimura, N., DaSalla, C. S., Hanakawa, T., Sato, M. A., and Koike, Y. (2012). Reconstruction of flexor and extensor muscle activities from electroencephalography cortical currents. *Neuroimage 59*(2), 1324-1337.

Yoshimura, N., Tsuda, H., Kawase, T., Kambara, H., and Koike, Y. (2017). Decoding finger movement in humans using synergy of EEG cortical current signals. *Sci. Rep.* 7(1), 11382.

Zander, T. O., and Kothe, C. (2011). Towards passive brain-computer interfaces: applying brain-computer interface technology to human-machine systems in general. *J. Neural. Eng.* 8(2), 025005.

Zhang, J., Sudre, G., Li, X., Wang, W., Weber, D. J., and Bagic, A. (2011). Clustering linear discriminant analysis for MEG-based brain computer interfaces. *IEEE Trans. Neural. Syst. Rehabil. Eng.* 19(3), 221-231.

Publications related to this study

Kim, H., Yoshimura, N., & Koike, Y. (2019). Classification of movement intention using independent components of premovement EEG. *Frontiers in human neuroscience*, *13*, 63.

Kim, H., Yoshimura, N., & Koike, Y. (2019). Characteristics of kinematic parameters in decoding intended reaching movements using electroencephalography (EEG). *Frontiers in neuroscience*, *13*.